



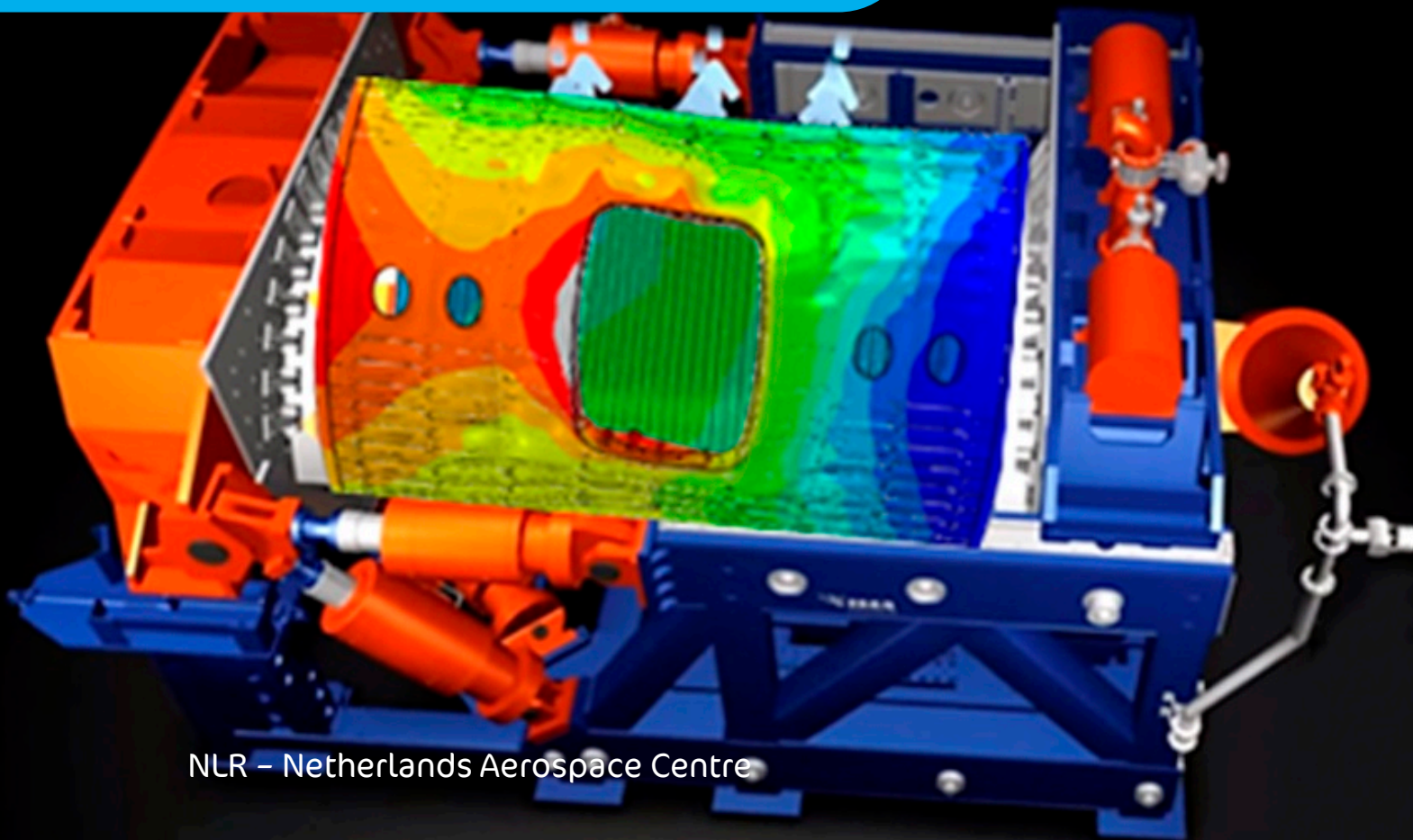
Dedicated to innovation in aerospace

NLR-TP-2016-172 | January 2017

Validation and correlation of aircraft composite fuselage structure models

Preliminary results

CUSTOMER: NLR



NLR – Netherlands Aerospace Centre

Netherlands Aerospace Centre

NLR is a leading international research centre for aerospace. Bolstered by its multidisciplinary expertise and unrivalled research facilities, NLR provides innovative and integral solutions for the complex challenges in the aerospace sector.

NLR's activities span the full spectrum of Research Development Test & Evaluation (RDT & E). Given NLR's specialist knowledge and facilities, companies turn to NLR for validation, verification, qualification, simulation and evaluation. NLR thereby bridges the gap between research and practical applications, while working for both government and industry at home and abroad.

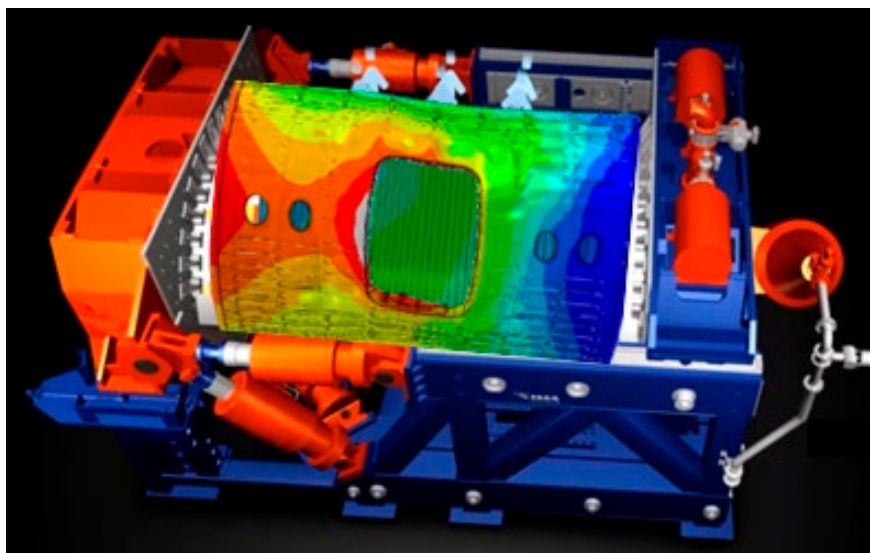
NLR stands for practical and innovative solutions, technical expertise and a long-term design vision. This allows NLR's cutting edge technology to find its way into successful aerospace programs of OEMs, including Airbus, Embraer and Pilatus. NLR contributes to (military) programs, such as ESA's IXV re-entry vehicle, the F-35, the Apache helicopter, and European programs, including SESAR and Clean Sky 2.

Founded in 1919, and employing some 650 people, NLR achieved a turnover of 73 million euros in 2014, of which three-quarters derived from contract research, and the remaining from government funds.

For more information visit: www.nlr.nl

Validation and correlation of aircraft composite fuselage structure models

Preliminary results



Problem area

NLR participates in the MAAXIMUS project (More Affordable Aircraft structure through eXtended, Integrated & Mature nUmerical Sizing) to develop capabilities for the fast development and right-first-time validation of a highly-optimized composite airframe. This is achieved through coordinated developments on a physical platform, by (1) developing and validating the appropriate composite technologies for low weight aircraft, and on a virtual platform, by (2) identifying faster and validating earlier the best solutions.

One of the investigations in MAAXIMUS deals with the reduction of time and costs needed for full-scale structural validation testing, which is usually done on fuselage barrel level. The aim is to achieve validation testing on a slightly lower level of the test pyramid, in particular on large fuselage panels that do include the critical and complex structural features of the aircraft fuselage.

REPORT NUMBER

NLR-TP-2016-172

AUTHOR(S)

W.J. Vankan
W.M. van den Brink
R. Maas

REPORT CLASSIFICATION

UNCLASSIFIED

DATE

January 2017

KNOWLEDGE AREA(S)

Computational Mechanics
and Simulation Technology

DESCRIPTOR(S)

panel test
CAD
finite element model
load identification
damage simulation

Description of work

The present paper describes a virtual testing model study of a large composite fuselage side panel. The focus of this study is to prepare for correlation analyses between the virtual and physical test results. Detailed representations of the loads and boundary conditions from the test rig are incorporated in the virtual testing model. Local structural responses in specific skin regions or in sub-components like frames are evaluated. The local analysis is done in high detail to efficiently capture local stress/strain states during virtual tests. Furthermore, the high detail enables the local test results to be effectively correlated with extensive physical test results.

Results and conclusions

To carry out the virtual test of the side panel, detailed finite element models (DFEMs) of the side panel and of the fuselage barrel are used. The panel DFEM assembly is derived from a detailed CAD model. Specifically, the procedures for the extraction of local strain results, which are needed for the validation and correlation with the physical test, are considered in this study. The issues in these procedures, due to the complexities of the very many part-instances in the virtual test model, are addressed. Because of the un-availability of the physical test data, the actual correlation analysis between virtual and physical test has not yet been done.

Applicability

The virtual testing approach used here can be applied to any large scale structural validation test, i.e. not only fuselage but any (primary) aircraft structure. The strain evaluation procedure presented here was applied specifically to composite structures, but the overall virtual testing approach is also applicable to metallic structures.

GENERAL NOTE

This report is based on a presentation held at the ECCOMAS-2016 Congress, Hersonissos, Greece, June 5-10, 2016.

NLR

Anthony Fokkerweg 2
1059 CM Amsterdam

p) +31 88 511 3113 f) +31 88 511 3210
e) info@nlr.nl i) www.nlr.nl



Dedicated to innovation in aerospace

NLR-TP-2016-172 | January 2017

Validation and correlation of aircraft composite fuselage structure models

Preliminary results

CUSTOMER: NLR

AUTHOR(S):

W.J. Vankan

W.M. van den Brink

R. Maas

Netherlands Aerospace Centre

Netherlands Aerospace Centre



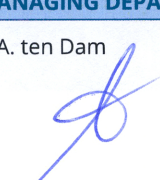
Netherlands Aerospace Centre

This report is based on a presentation held at the ECCOMAS-2016 Congress, Hersonissos, Greece, June 5-10, 2016.

The contents of this report may be cited on condition that full credit is given to NLR and the authors.

This publication has been refereed by the Advisory Committee AEROSPACE VEHICLES.

CUSTOMER	NLR
CONTRACT NUMBER	213371
OWNER	NLR
DIVISION NLR	Aerospace Vehicles
DISTRIBUTION	Unlimited
CLASSIFICATION OF TITLE	UNCLASSIFIED

APPROVED BY :																				
AUTHOR				REVIEWER				MANAGING DEPARTMENT												
W.J. Van kan 				A.J. de Wit 				A.A. ten Dam 												
DATE	1	5	0	2	1	7	DATE	1	6	0	2	1	7	DATE	1	7	0	2	1	7

Summary

The present paper describes the study of a virtual testing model of a large composite fuselage side panel. The focus of this study is to prepare for correlation analyses between virtual and physical test results of a large composite fuselage side panel test. Detailed representations of the loads and boundary conditions from the test rig are incorporated in the virtual testing model. Local structural responses in specific skin regions or in sub-components like frames are evaluated. The evaluation is carried out in high detail to efficiently capture local stress/strain states during tests and to effectively correlate with extensive physical test results. For the virtual test of the side panel, detailed finite element models (DFEMs) of the side panel and of the fuselage barrel are used. The panel DFEM assembly is derived from a detailed CAD model. Specifically the procedures for the extraction of local strain results, which are needed for the validation and correlation with the physical test, are considered in this study. The issues in these procedures, due to the complexities of the many part-instances in the virtual test model, are addressed. Because of the un-availability of the physical test data, the actual correlation analysis between virtual and physical test has not yet been done.

This page is intentionally left blank.

Contents

Abbreviations	6
1 Introduction	9
2 Overview of the study	10
3 Panel design	13
4 Panel DFEM creation from CAD	16
4.1 Model simplifications and de-featuring	16
4.2 Part properties	18
4.3 Panel DFEM assembly, ties, constraints	20
4.4 Boundary conditions and load introductions	22
4.5 Load cases and static analyses	24
4.6 Loads identification	25
4.7 Strains evaluation	27
4.7.1 Direct strain evaluation	28
4.7.2 Incorporation of strain gauges in DFEM	29
4.7.3 Strain gauges as sub-model of the DFEM	29
5 Results from strain evaluation study	31
6 Conclusions	40
7 References	41

Abbreviations

ACRONYM	DESCRIPTION
2D	Two dimensional
3D	Three dimensional
α	load factors
Alu	Aluminium
BC	Boundary condition
c-sys	Coordinate system
CAD	Computer aided design
DFEM	detailed finite element model
DNW	German-Dutch Wind Tunnels
dof	Degrees of freedom
dP	differential pressure
DSS	door surround structure
ϵ	Strain
FE	finite element
FEM	finite element method
GFRP	Glass fibre reinforced plastic
GPa	Giga Pascal
HEX	Hexahedral
ILSS	Inter-laminar shear strength
IPSS	In-plane shear strength
k	Kilo
LBL	Lateral bending left
LBR	Lateral bending right
LBLdP	pressurized lateral bending left
LBRdP	pressurized lateral bending right
LC	Load case
M	Mega
MAAXIMUS	More Affordable Aircraft structure through eXtended, Integrated & Mature nUmerical Sizing
MPa	Mega Pascal
NCF	non-crimp fabric
NLR	Netherlands Aerospace Centre
PAX	passengers
PEEK	Polyetheretherketone
R^2	coefficient of determination
RTM	resin transfer moulding

ACRONYM	DESCRIPTION
SG	Strain gauge
TET	Tetrahedral
UD	Uni-directional
VBD	vertical bending down
VBU	vertical bending up
VBDdP	pressurized vertical bending down
VBUDP	pressurized vertical bending up
XMBRS	Cross members

This page is intentionally left blank.

1 Introduction

In the development of composite fuselage for large aircraft, validation of new composite design and material technologies is ultimately done by full-scale testing on fuselage barrel level. To reduce time and costs needed for such tests, full-scale validation is aimed to be done on a slightly lower level of the test pyramid, typically on large fuselage panels that do include the critical and complex structural features such as circumferential or longitudinal joints, PAX door and the corresponding door surround structure or representative floor structures. Such tests require advanced and complex test rigs with sufficient flexibility to accurately impose the required loads and boundary conditions on the considered test article. Furthermore, the test rigs have to allow for proper load introduction of shear and bending loads, airtight sealing to allow for pressurisation loading, correct fixation and loading of stringers, frames and floor beams. Such advanced test rigs have been developed for large panels and for a variety of loads and test conditions, for example at IMA (IMA Materialforschung und Anwendungstechnik GmbH, Germany). This panel level test rig must introduce the loads into the test article in such a way that the structural response of the panel is consistent with the full-scale testing of the fuselage barrel level, which is as close as possible to the in-flight situation. To achieve this, accurate modelling and analyses of the detailed behaviour of the panel in the test rig are applied through extensive model studies ("virtual testing") as commonly used at Airbus [2] and in Maaximus where the term mainly refers to simulations for the purpose of physical tests using large finite element (FE) models that take into account the relevant aspects of the test rig.

This paper presents a virtual testing study of a large composite fuselage side panel using a detailed finite element model (DFEM) of this side panel. Proper loads and boundary conditions for the test rig have been determined with this DFEM by a loads identification study. In this study the test rig actuator loads are incorporated in the DFEM and are then tuned such that the model responses (strains or section forces in many locations of the panel structure) correspond as good as possible with the responses that were found from the DFEM simulation of the barrel tests. These barrel test simulations were performed for a set of representative barrel level static load cases (like lateral and vertical bending and internal pressure). Once the panel level loads (i.e. the test rig actuator loads) are determined for all the considered load cases, the structural responses of the panel DFEM can be evaluated. These responses are determined in different locations than for the loads identification. The reason for this is that these responses shall be correlated to the measured responses from the panel in the physical test rig, i.e. the strain gauge responses. To achieve proper correlations with the physical test data, these strain responses must be accurately determined from the panel DFEM, i.e. the virtual test. Typically, small details like the exact positions and orientations of the strain gauges on the inner and outer surfaces of the panel's sub-structures (i.e. skin, frames, stringers etc.) must be defined in high precision in the panel DFEM. The modelling methods and evaluation procedures for this highly detailed definition of strain gauges and accurate strain data extraction will be described in this paper. As such, these detailed strain data from the DFEM can be used for validation and correlation of the local structural model responses by comparison with the local measurements from the physical tests. It should be noted that the actual comparison with physical test data cannot be presented because the test results are not yet available.

2 Overview of the study

In the MAAXIMUS project, the development of a test procedure for a large fuselage panel is considered. This panel does include the critical and complex structural features such as the PAX door and the corresponding door surround structure (DSS) as well as representative floor structures. Furthermore, the panel includes some parts that were produced with new developments for part manufacturing. The panel test procedure requires an advanced and complex test rig with sufficient flexibility to accurately impose the required loads and boundary conditions on the considered test article. Proper load introduction of shear and bending loads, airtight sealing to allow for pressurisation loading, correct fixation and loading of stringers, frames and floor beams shall be ensured. The advanced test rig that will be applied in MAAXIMUS is available at IMA and has been developed for large panels of wide-body aircraft fuselage and for high versatility in loading and test conditions [1] (see Figure 1).



Figure 1: The test rig to be used for the MAAXIMUS panel: IMA's fuselage test system V4. [1]

One of the main performance criteria for this advanced panel level test rig is to introduce loads into the test article in such a way that the structural response in the test rig is fully consistent with the full-scale testing on fuselage barrel level, which is as close as possible to the in-flight situation (Figure 2).

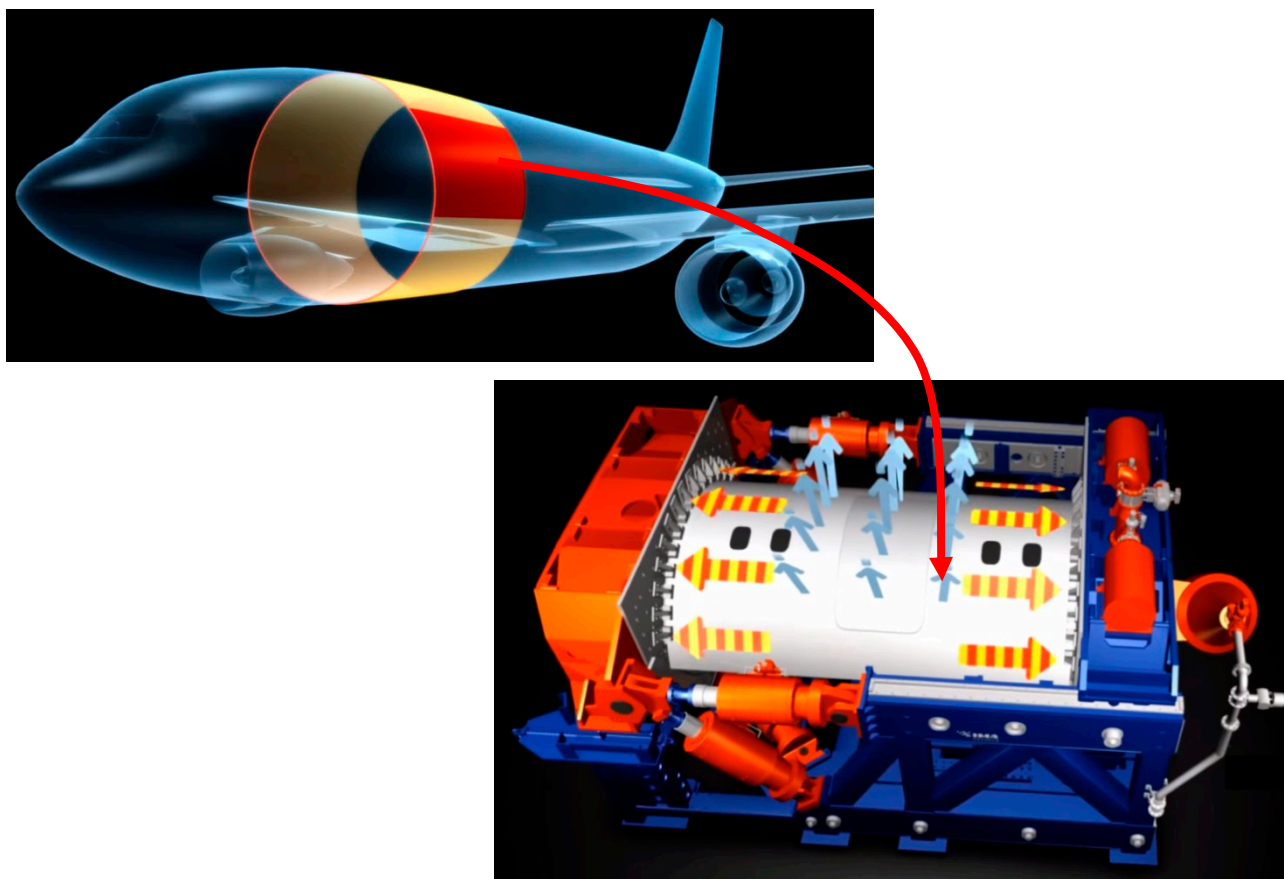


Figure 2: Illustration of aircraft front-fuselage barrel (upper figure), and panel cut-out being tested in a large fuselage panel test rig (lower figure) as developed at IMA [1]

To capture the behaviour of the structure in the full-scale barrel test, accurate modelling and analyses of the detailed behaviour of the barrel structure are applied. This is achieved through extensive model studies ("virtual testing") using large finite element (FE) models [2] for highly detailed representation of aircraft fuselage structures Figure 3 (so-called detailed finite element models (DFEMs)).

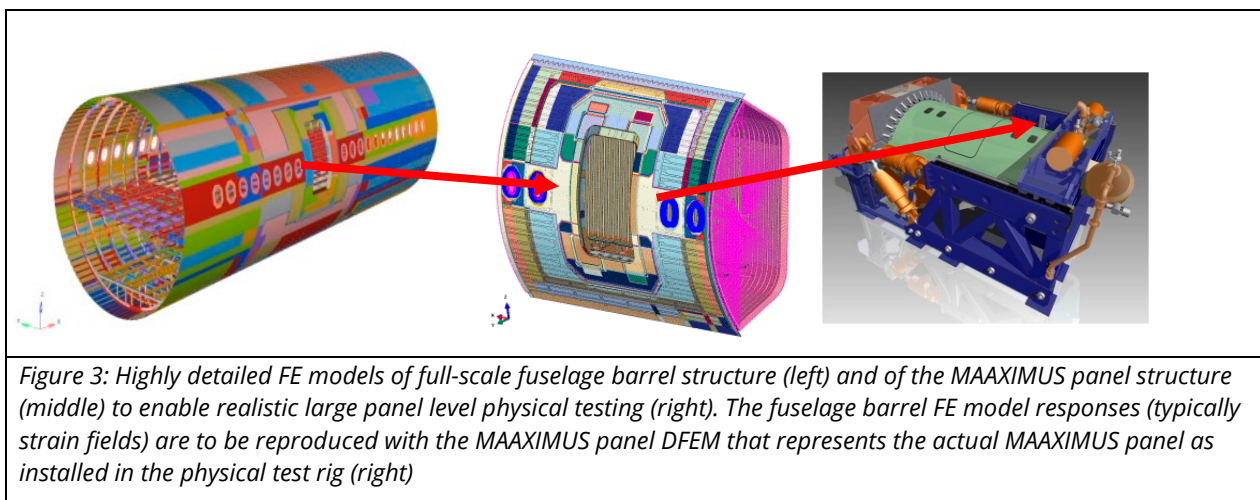


Figure 3: Highly detailed FE models of full-scale fuselage barrel structure (left) and of the MAAXIMUS panel structure (middle) to enable realistic large panel level physical testing (right). The fuselage barrel FE model responses (typically strain fields) are to be reproduced with the MAAXIMUS panel DFEM that represents the actual MAAXIMUS panel as installed in the physical test rig (right)

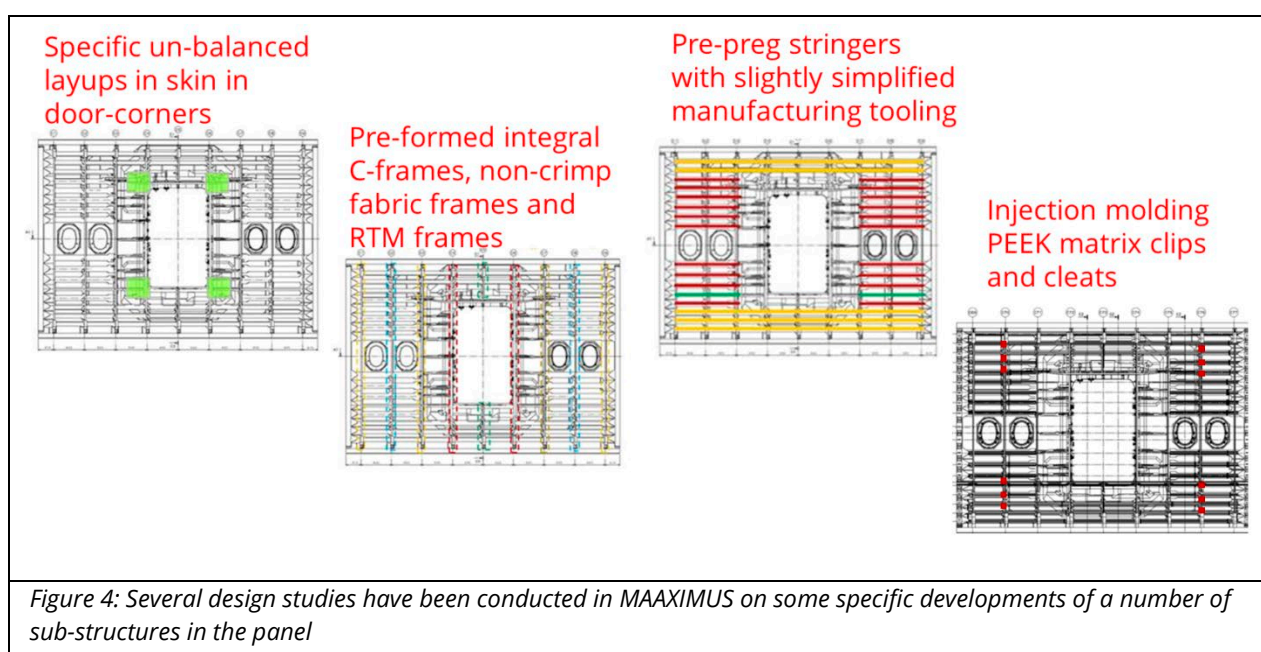
The barrel level FE analyses are used to capture the responses to the load cases, which are defined on barrel level. These barrel level load cases are based on 9 static aircraft load cases, including lateral and vertical bending and internal pressure. The MAAXIMUS panel DFEM as developed in this work

represents the actual MAAXIMUS panel as installed in the physical test rig. Therefore, this panel DFEM also contains the local reinforcements for load introductions and the actuation forces and boundary conditions as applied in the test rig. This model is used for the identification of the test rig loads by correlation of extensive sets of local strains and force flows with the fuselage barrel FE model.

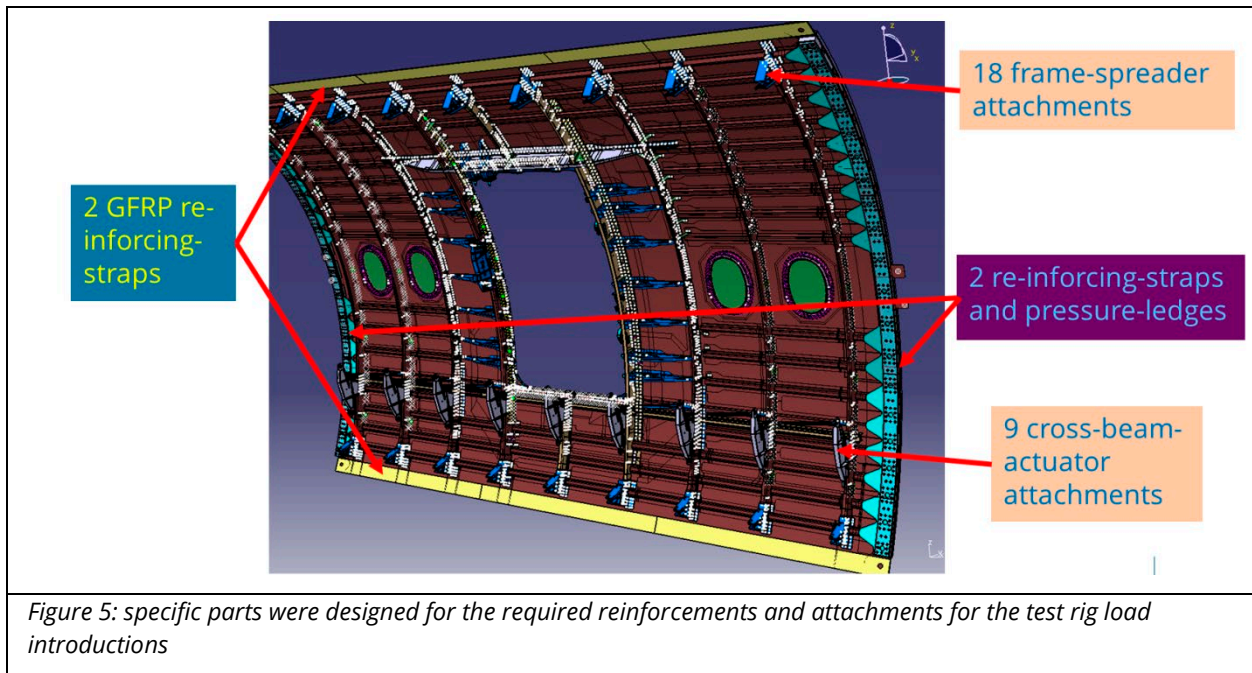
For the virtual testing analysis of the side panel, the DFEMs of both the side panel and the fuselage barrel are needed. The focus in this study is mainly on the development and the analyses of the panel DFEM; the modelling details of the barrel DFEM are comparable to those of the panel.

3 Panel design

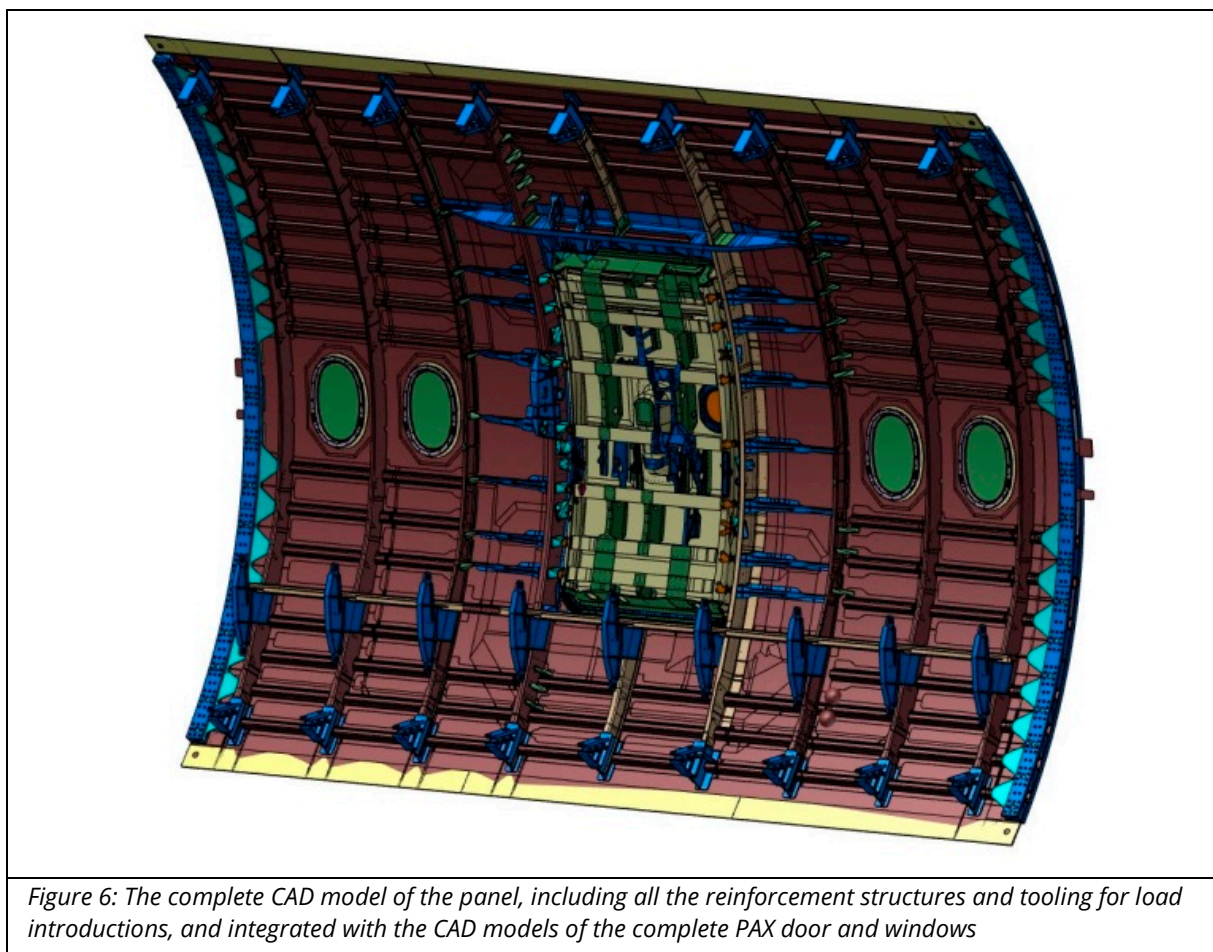
The design of the MAAXIMUS panel model is representative for a PAX door region of a wide-body fuselage. Several design studies have been conducted in MAAXIMUS on some specific developments of a number of sub-structures in the panel. For example in the PAX door corners, specific composite layups were applied to achieve strain reductions and manufacturing advantages. Also several different frame developments were applied in the panel, including pre-formed integral C-frames, non-crimp fabric (NCF) frames and RTM frames. Some stringer developments were applied in the panel, allowing for slightly simplified manufacturing tooling. Also some material developments were applied to clips and cleats using injection molding PEEK matrix (see also [3]). These structural developments and their indicative locations on the panel are illustrated in Figure 4.



Besides these specific developments of some of the panel's sub-structures, also specific parts were designed for the required reinforcements and attachments for the test rig load introductions (see Figure 5). For example, the reinforcing-straps and pressure-ledges at the curved panel edges, the GFRP-straps at the straight panel edges, the frame-spreader attachments and the cross-beam-actuator attachments were added.



The resulting design of the complete MAAXIMUS panel, including all reinforcements and attachments, has been fully defined in a CATIA V5 [4] CAD model, as shown in Figure 6. This CAD model is the basis for the development of the virtual testing DFEM of the MAAXIMUS panel.



Because the intended tests do include pressurisation of the panel, the test article must also include the PAX door and window components. For illustration, these components are integrated into the panel CAD model as shown in Figure 6. However, because the door and windows do not (or hardly) contribute to the in-plane stiffness of the fuselage, a detailed representation of these parts is not essential for the panel DFEM. Therefore, the incorporation of the PAX door and windows in the DFEM will be strongly simplified to include their pressure forces into the structure, as will be explained in Section 4.3. It should be noted that the door surround structure and the window frames are incorporated in detail into the panel DFEM.

4 Panel DFEM creation from CAD

The panel DFEM is based on the panel design as given by the detailed CAD model developed in CATIA V5. The panel DFEM assembly is derived from the detailed CAD model, mainly for its geometry, assembly and properties.

4.1 Model simplifications and de-featuring

The panel CAD contains a large number (approx. 1000) of large and small detailed parts, ranging from the full panel skin part, to small nuts and bolts (Figure 7). In the DFEM creation a selection was made of the most important parts that are to be incorporated. Typically, the small parts like many nuts, bolts, washers etc. have not been included in the DFEM but are replaced by fasteners or ties (connections between parts) in the DFEM. A global overview of the parts in the CAD and the way in which these parts have been included in the DFEM is given.

Feature name	Description	Integration in Abaqus	Representation in Abaqus	Abaqus part mapping	Material	Layer
MGY-MAAXIMUS.1\MGY BARREL1BR2	datum lines frames, stringers, door	no				
MGY-MAAXIMUS.1\MGY MAAXIMUS	datum lines side panel	no				
REFERENCE B1BR2.1\FRAMES.1\V8B57460000000-C71.1\64.1\V8B57489020400	frame stiffener near floor beam	yes	shell	1	aluminium	45/90/-45/0/45/-45/0/0/90/0/0/-45/45/0/-45/90/45
REFERENCE B1BR2.1\FRAMES.1\V8B57460000000-C72.1\76.1\PartBody	cleat clip	yes	shell	2	composite	45/90/-45/0/45/-45/0/0/90/0/0/-45/45/0/-45/90/45
REFERENCE B1BR2.1\FRAMES.1\V8B57460000000-C72.1\76.2\PartBody	cleat clip	yes	shell	3	composite	45/90/-45/0/45/-45/0/0/90/0/0/-45/45/0/-45/90/45
REFERENCE B1BR2.1\FRAMES.1\V8B57460000000-C72.1\76.3\PartBody	cleat clip	yes	shell	4	composite	45/90/-45/0/45/-45/0/0/90/0/0/-45/45/0/-45/90/45
REFERENCE B1BR2.1\FRAMES.1\V8B57460000000-C72.1\76.4\PartBody	cleat clip	yes	shell	5	composite	45/90/-45/0/45/-45/0/0/90/0/0/-45/45/0/-45/90/45
REFERENCE B1BR2.1\FRAMES.1\V8B57460000000-C72.1\76.5\PartBody	cleat clip	yes	shell	6	composite	45/90/-45/0/45/-45/0/0/90/0/0/-45/45/0/-45/90/45
REFERENCE B1BR2.1\FRAMES.1\V8B57460000000-C72.1\76.6\PartBody	cleat clip	yes	shell	7	composite	45/90/-45/0/45/-45/0/0/90/0/0/-45/45/0/-45/90/45
REFERENCE B1BR2.1\FRAMES.1\V8B57460000000-C72.1\76.7\PartBody	cleat clip	yes	shell	8	composite	45/90/-45/0/45/-45/0/0/90/0/0/-45/45/0/-45/90/45
REFERENCE B1BR2.1\FRAMES.1\V8B57460000000-C72.1\76.8\PartBody	cleat clip	yes	shell	9	composite	45/90/-45/0/45/-45/0/0/90/0/0/-45/45/0/-45/90/45
REFERENCE B1BR2.1\FRAMES.1\V8B57460000000-C72.1\76.9\PartBody	cleat clip	yes	shell	10	composite	45/90/-45/0/45/-45/0/0/90/0/0/-45/45/0/-45/90/45
REFERENCE B1BR2.1\FRAMES.1\V8B57460000000-C72.1\76.10\PartBody	cleat clip	yes	shell	11	composite	45/90/-45/0/45/-45/0/0/90/0/0/-45/45/0/-45/90/45
REFERENCE B1BR2.1\FRAMES.1\V8B57460000000-C73.1\44.7\V8B57474120400	cleat clip	yes	shell	12	composite	45/90/-45/0/45/-45/0/0/90/0/0/-45/45/0/-45/90/45
REFERENCE B1BR2.1\FRAMES.1\V8B57460000000-C73.1\84.1\PartBody	cleat clip	yes	shell	13	composite	45/90/-45/0/45/-45/0/0/90/0/0/-45/45/0/-45/90/45
REFERENCE B1BR2.1\FRAMES.1\V8B57460000000-C73.1\86.1\V8B57485030000	cleat clip	yes	shell	14	composite	45/90/-45/0/45/-45/0/0/90/0/0/-45/45/0/-45/90/45
REFERENCE B1BR2.1\FRAMES.1\V8B57460000000-C73.1\88.1\V8B57474121400	cleat clip	yes	shell	15	composite	45/90/-45/0/45/-45/0/0/90/0/0/-45/45/0/-45/90/45
REFERENCE B1BR2.1\FRAMES.1\V8B57460000000-C73.1\90.1\PartBody	frame stiffener near floor beam	yes	shell	16	aluminium	45/90/-45/0/45/-45/0/0/90/0/0/-45/45/0/-45/90/45
REFERENCE B1BR2.1\FRAMES.1\V8B57460000000-C73.1\92.1\PartBody	cleat clip	yes	shell	17	composite	45/90/-45/0/45/-45/0/0/90/0/0/-45/45/0/-45/90/45
REFERENCE B1BR2.1\FRAMES.1\V8B57460000000-C73.1\94.1\PartBody	cleat clip	yes	shell	18	composite	45/90/-45/0/45/-45/0/0/90/0/0/-45/45/0/-45/90/45
REFERENCE B1BR2.1\FRAMES.1\V8B57460000000-C74.1\76.6\PartBody	cleat clip	yes	shell	19	composite	45/90/-45/0/45/-45/0/0/90/0/0/-45/45/0/-45/90/45
REFERENCE B1BR2.1\FRAMES.1\V8B57460000000-C74.1\76.7\PartBody	cleat clip	yes	shell	20	composite	45/90/-45/0/45/-45/0/0/90/0/0/-45/45/0/-45/90/45
REFERENCE B1BR2.1\FRAMES.1\V8B57460000000-C74.1\76.8\PartBody	cleat clip	yes	shell	21	composite	45/90/-45/0/45/-45/0/0/90/0/0/-45/45/0/-45/90/45
REFERENCE B1BR2.1\FRAMES.1\V8B57460000000-C74.1\76.9\PartBody	cleat clip	yes	shell	22	composite	45/90/-45/0/45/-45/0/0/90/0/0/-45/45/0/-45/90/45
REFERENCE B1BR2.1\FRAMES.1\V8B57460000000-C74.1\76.10\PartBody	cleat clip	yes	shell	23	composite	45/90/-45/0/45/-45/0/0/90/0/0/-45/45/0/-45/90/45
REFERENCE B1BR2.1\FRAMES.1\V8B57460000000-C74.1\78.1\PartBody	cleat clip	yes	shell	24	composite	45/90/-45/0/45/-45/0/0/90/0/0/-45/45/0/-45/90/45
REFERENCE B1BR2.1\FRAMES.1\V8B57460000000-C74.1\78.2\PartBody	cleat clip	yes	shell	25	composite	45/90/-45/0/45/-45/0/0/90/0/0/-45/45/0/-45/90/45
REFERENCE B1BR2.1\FRAMES.1\V8B57460000000-C74.1\78.3\PartBody	cleat clip	yes	shell	26	composite	45/90/-45/0/45/-45/0/0/90/0/0/-45/45/0/-45/90/45
REFERENCE B1BR2.1\FRAMES.1\V8B57460000000-C74.1\78.4\PartBody	cleat clip	yes	shell	27	composite	45/90/-45/0/45/-45/0/0/90/0/0/-45/45/0/-45/90/45
REFERENCE B1BR2.1\FRAMES.1\V8B57460000000-C74.1\78.5\PartBody	cleat clip	yes	shell	28	composite	45/90/-45/0/45/-45/0/0/90/0/0/-45/45/0/-45/90/45
REFERENCE B1BR2.1\FRAMES.1\V8B57460000000-C75.1\66.1\V8B57489020600	frame stiffener near floor beam	yes	shell	29	aluminium	45/90/-45/0/45/-45/0/0/90/0/0/-45/45/0/-45/90/45
REFERENCE B1BR2.1\FRAMES.1\V8B57460000000-C75.1\74.1\PartBody	intercostal	yes	solid	30	aluminium	
REFERENCE B1BR2.1\FRAMES.1\V8B57460000000-C75.1\112.1\PartBody	intercostal	yes	solid	31	aluminium	
REFERENCE B1BR2.1\FRAMES.1\V8B57460000000-C75.1\140.1\V8B57472520200	axial stiffener under frame	yes	shell	32	aluminium	
REFERENCE B1BR2.1\FRAMES.1\V8B57460000000-C75.1\142.1\V8B57473320600	rib above door	no				
REFERENCE B1BR2.1\FRAMES.1\V8B57460000000-C75.1\144.1\V8B57473321000	rib above door	no				
REFERENCE B1BR2.1\FRAMES.1\V8B57460000000-C75.1\146.1\V8B57474122800.1\V8 cleat clip	cleat clip	yes	shell	35	composite	45/90/-45/0/45/-45/0/0/90/0/0/-45/45/0/-45/90/45
REFERENCE B1BR2.1\FRAMES.1\V8B57460000000-C75.1\146.1\V8B57474122400.1\V8 cleat clip	cleat clip	yes	shell	36	composite	45/90/-45/0/45/-45/0/0/90/0/0/-45/45/0/-45/90/45
REFERENCE B1BR2.1\FRAMES.1\V8B57460000000-C75.1\148.1\V8B57472620200\V88 cleat clip	cleat clip	yes	shell	37	composite	45/90/-45/0/45/-45/0/0/90/0/0/-45/45/0/-45/90/45
REFERENCE B1BR2.1\FRAMES.1\V8B57460000000-C75.1\148.1\V8B57472620600\V88 cleat clip	cleat clip	yes	shell	38	composite	45/90/-45/0/45/-45/0/0/90/0/0/-45/45/0/-45/90/45
REFERENCE B1BR2.1\FRAMES.1\V8B57460000000-C75.1\138.1\V8B57472520000	axial stiffener under frame	yes	shell	39	aluminium	
REFERENCE B1BR2.1\FRAMES.1\V8B57460000000-C75.1\150.1\V8B57474220000	cleat clip	yes	shell	40	composite	45/90/-45/0/45/-45/0/0/90/0/0/-45/45/0/-45/90/45

Figure 7: Overview of a small extract from the large list of about 1000 detailed parts in the panel CAD model. Only a limited set of about 200 parts were adopted in the panel DFEM

The detailed definitions of the panel structure in the CAD model are based on 3D solid geometric representation in order to achieve sufficiently accurate representation and positioning in the CAD model assembly. Because many parts in the panel are thin-walled structures, the DFEM representation of these parts is simplified to the mid-surface shell representation. In particular, the shell instead of solid representation of the large thin structures like skin, stringers and frames contribute to the reduction of overall model size (Figure 8).

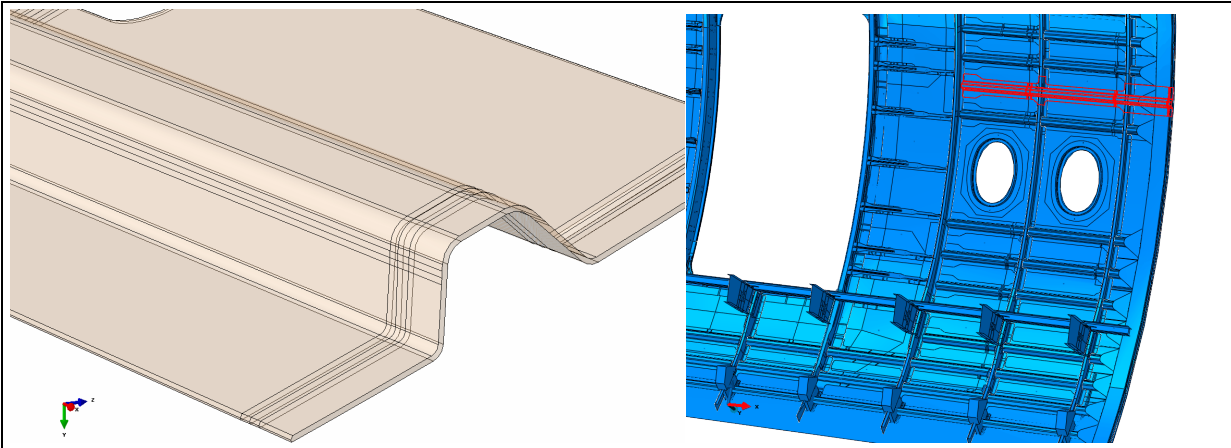
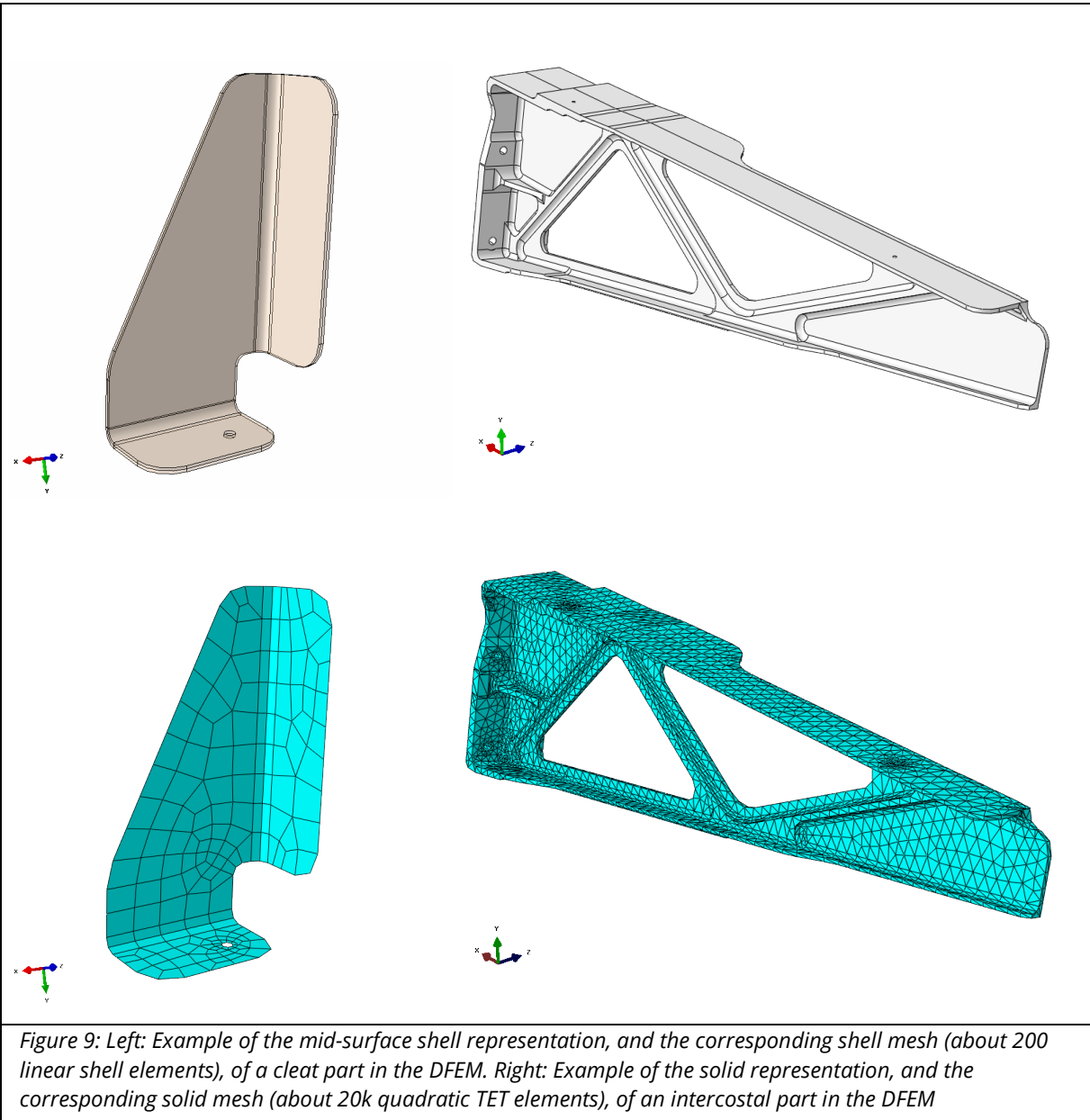


Figure 8: Example of the simplification of a hat-stringer part from solid representation as defined in the CAD to its surface shell representation in the DFEM (left: the bottom-surface of the solid stringer geometry is used for its shell representation; right: the shell-part instance of the stringer in the DFEM assembly)

Some further simplification and de-featuring is applied in the CAD to DFEM transfer (Figure 9). For example, by removing some small holes and simplifying some less significant parts (like some individual nuts and bolts). The DFEM is developed in the FE software ABAQUS [5], which offers specific functions (like mid-surface identification tools) to efficiently implement these simplifications.



4.2 Part properties

The parts in the DFEM are made of different materials and have different properties. The main materials used are carbon composites, aluminium and steel. Furthermore, glass-fibre composites are used for a few parts like the straight edge-straps reinforcements and titanium for some small parts like the door stops. Clearly, the main parts like the panel skin, frames and stringers are made of carbon composites. Different composite layups are used, each of which has been defined in the DFEM. The main aluminium parts are the cross- and floor beams, sill and lintel, intercostals, window frames and the curved edge-straps reinforcements. The main steel parts are for the load introductions of the frame spreaders. An overview of the main materials used in the panel DFEM is given in Figure 10.

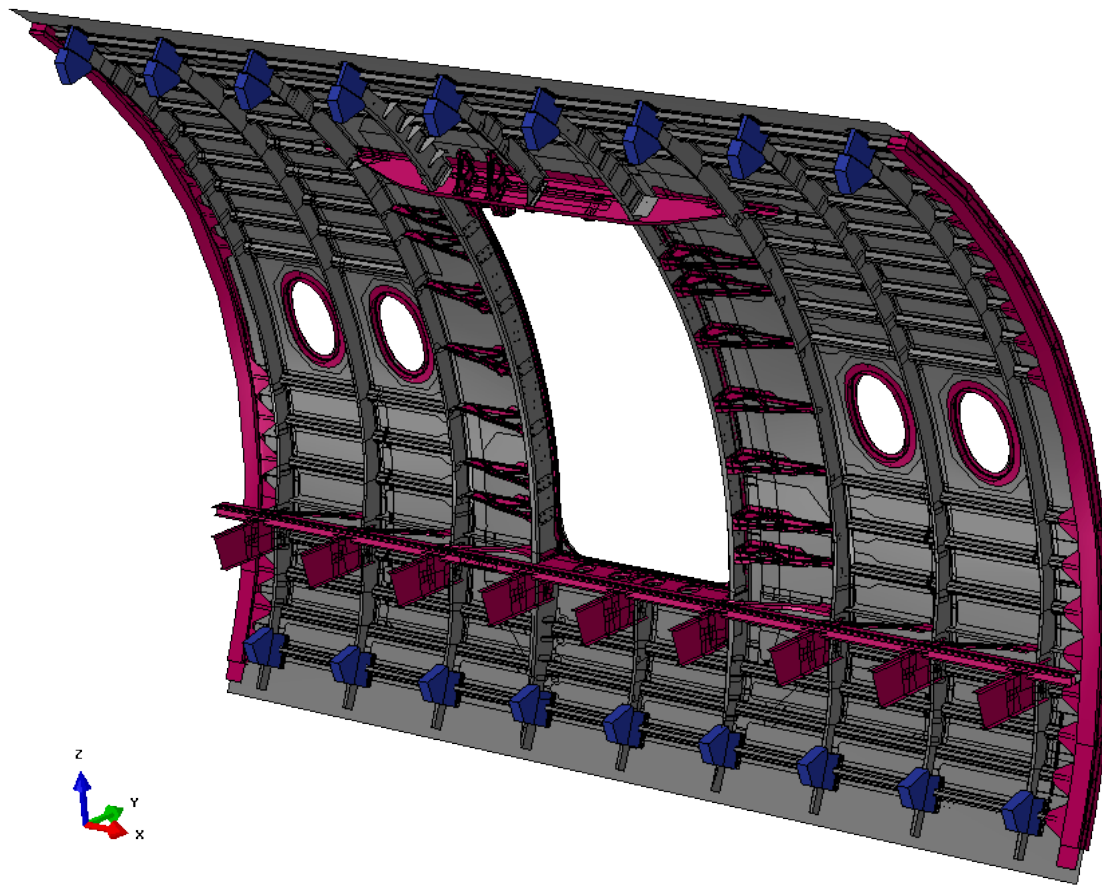
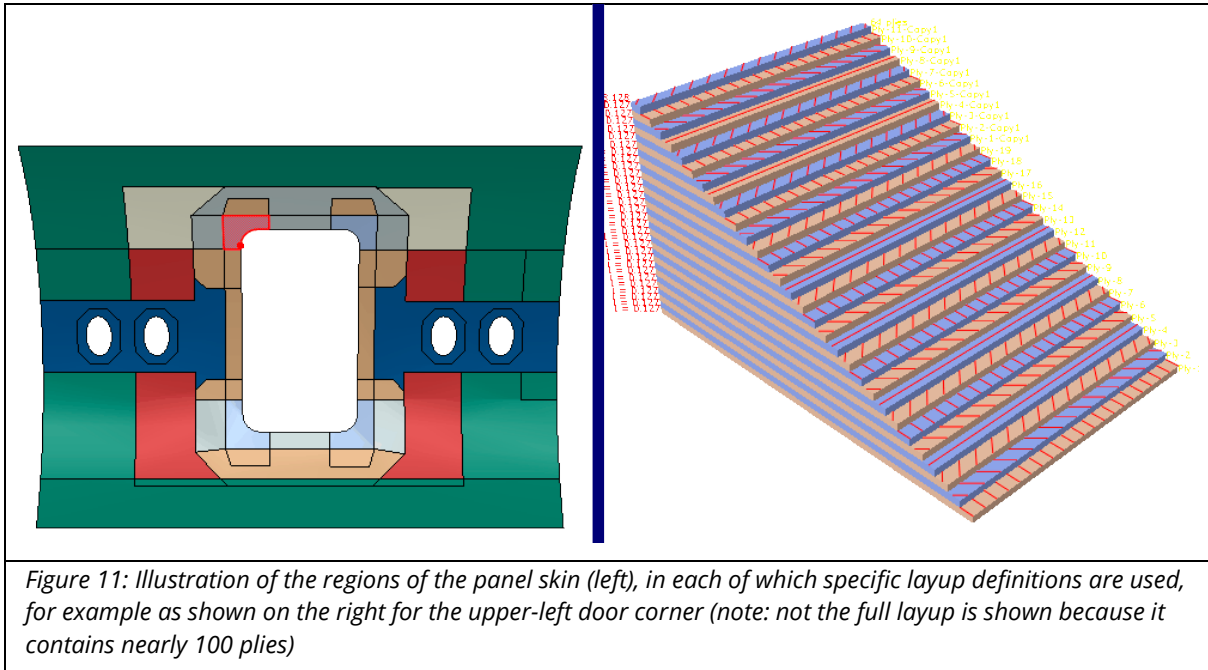


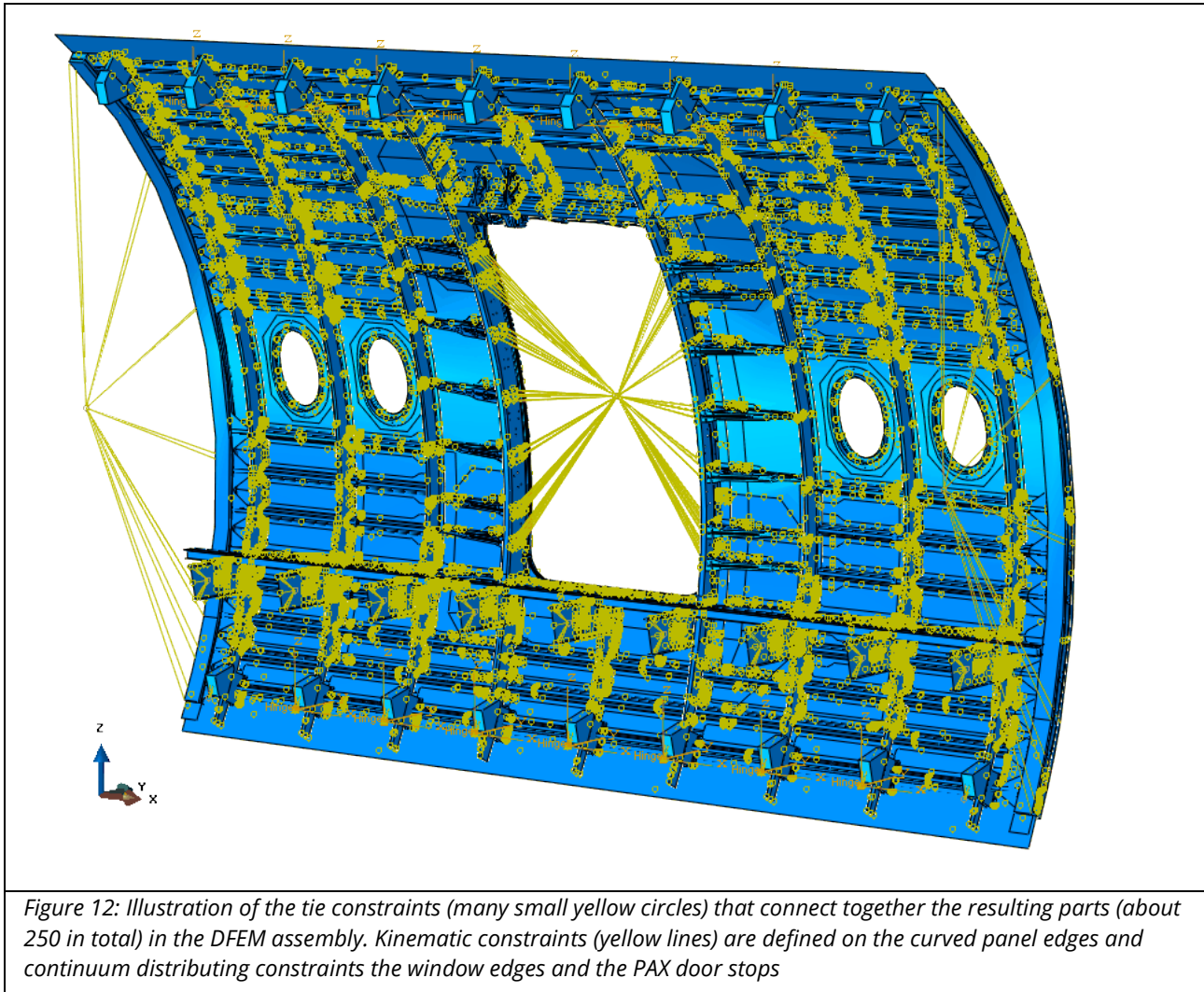
Figure 10: Main materials used in the panel DFEM (not all parts are shown here): grey is used for carbon composite, purple for Alu, blue for steel

The layup definitions of the composite parts are specific for different regions of the parts. For example, the skin has been subdivided into multiple regions in each of which specific layups are defined (see Figure 11). Obviously, the skin thickness varies significantly, ranging from about 3mm in the more peripheral skin regions up to about 12mm near the PAX door. Similarly, for the other composite parts such specific layup definitions are used. The main properties of the carbon UD ply of the HexPly M21/IMA material are approximately: 150GPa tension/compression modulus, 5GPa in-plane shear modulus, 2500MPa tension strength, 1500MPa compression strength, 100MPa IPSS/ ILSS [6].



4.3 Panel DFEM assembly, ties, constraints

All the resulting parts (about 250 in total) in the DFEM are properly positioned in the assembly and connected together with tie constraints (Figure 12). Also continuum distributing constraints [5] are defined on the curved panel edges, the window edges and the PAX door stops. These constraints on the windows and PAX door are used to transfer the pressure loads from windows and PAX door, resp., in the case of internal pressure load cases. This simplification allows for incorporation of the loads in an efficient way and is representative, because the in-plane stiffness contributions of windows and PAX door to the panel structure can be neglected.



All parts' properties (like materials, composite layups) and meshes (2D shells and 3D solids) are assigned on part level. Parts are meshed mostly with linear elements, yielding a total mesh for the assembly of about 1100k elements and 1.1M nodes for the full DFEM assembly (see Figure 13) and an FE problem size of approximately 4.6Mdof.

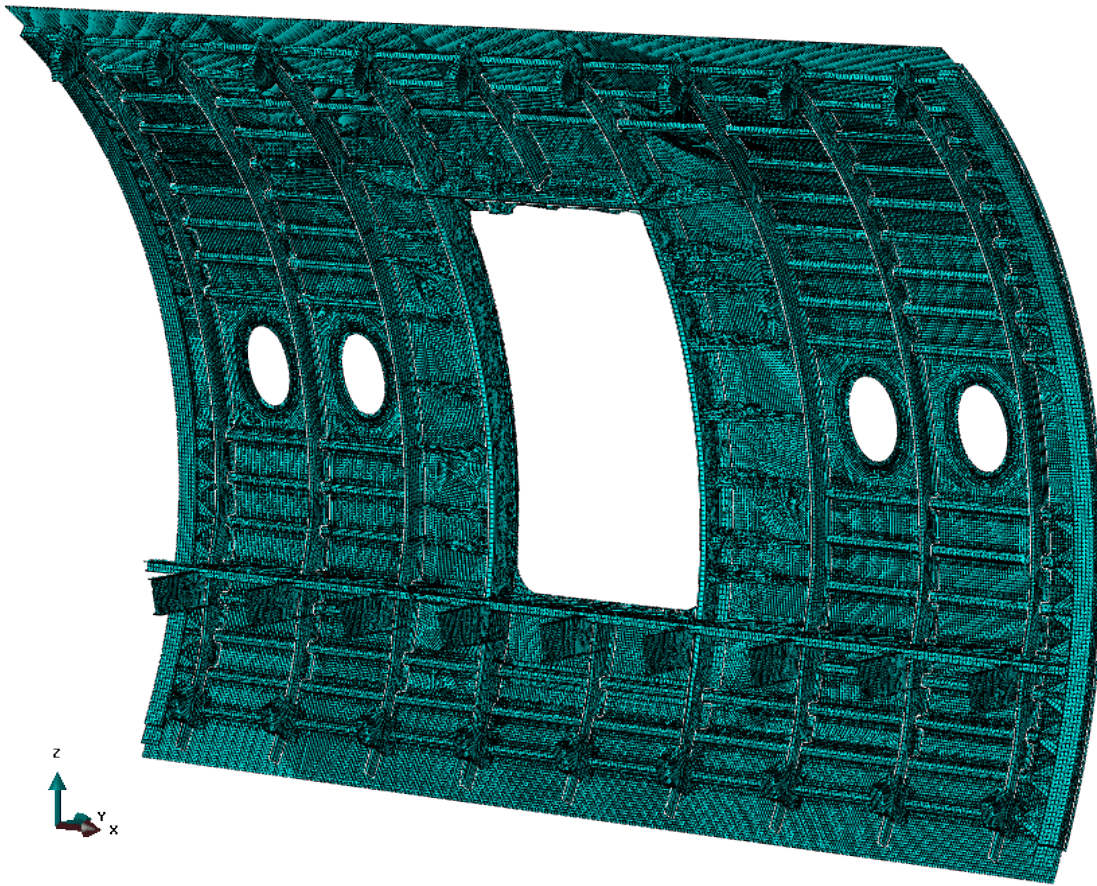
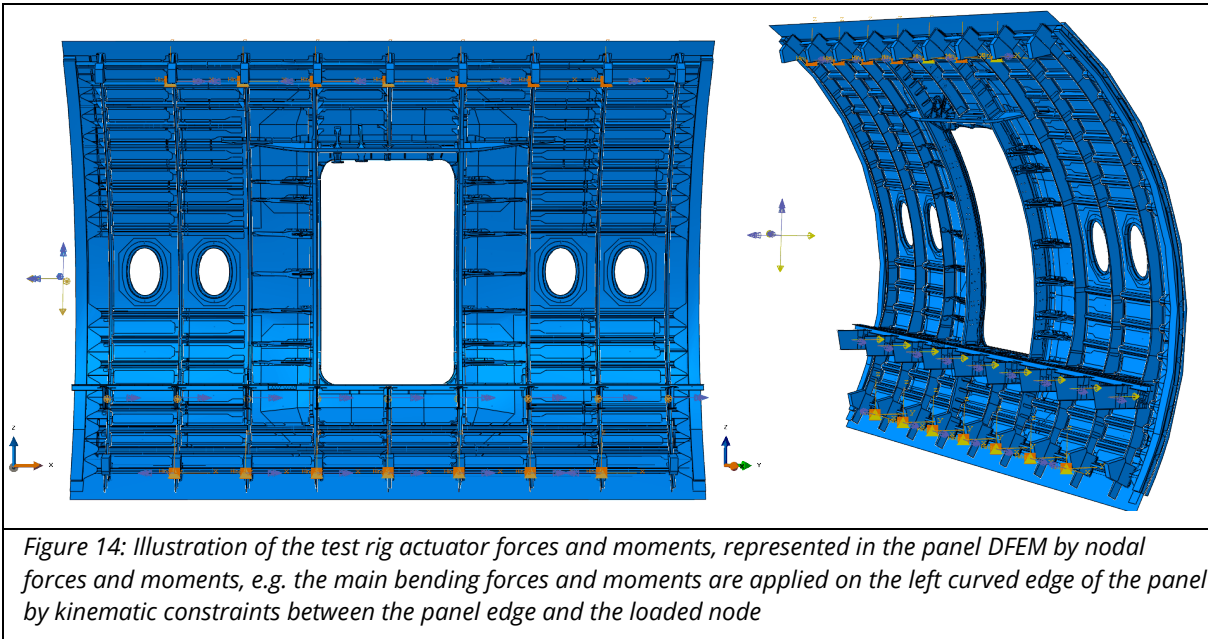


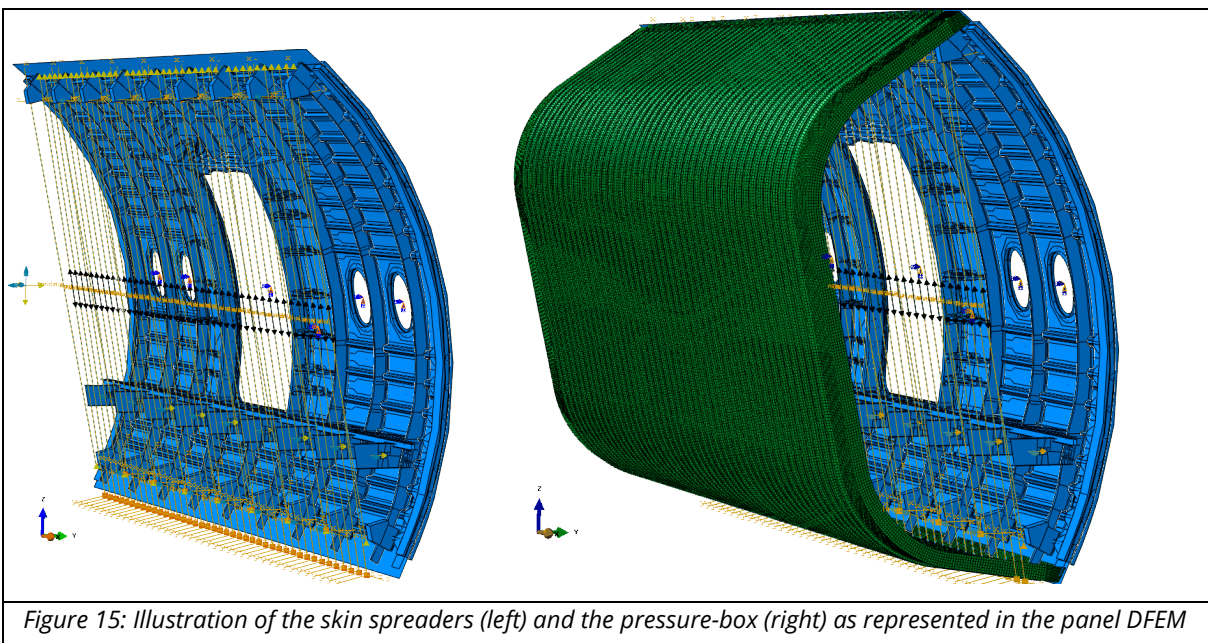
Figure 13: FE mesh of the full DFEM assembly containing in total approximately 1100k elements and 1.1M nodes

4.4 Boundary conditions and load introductions

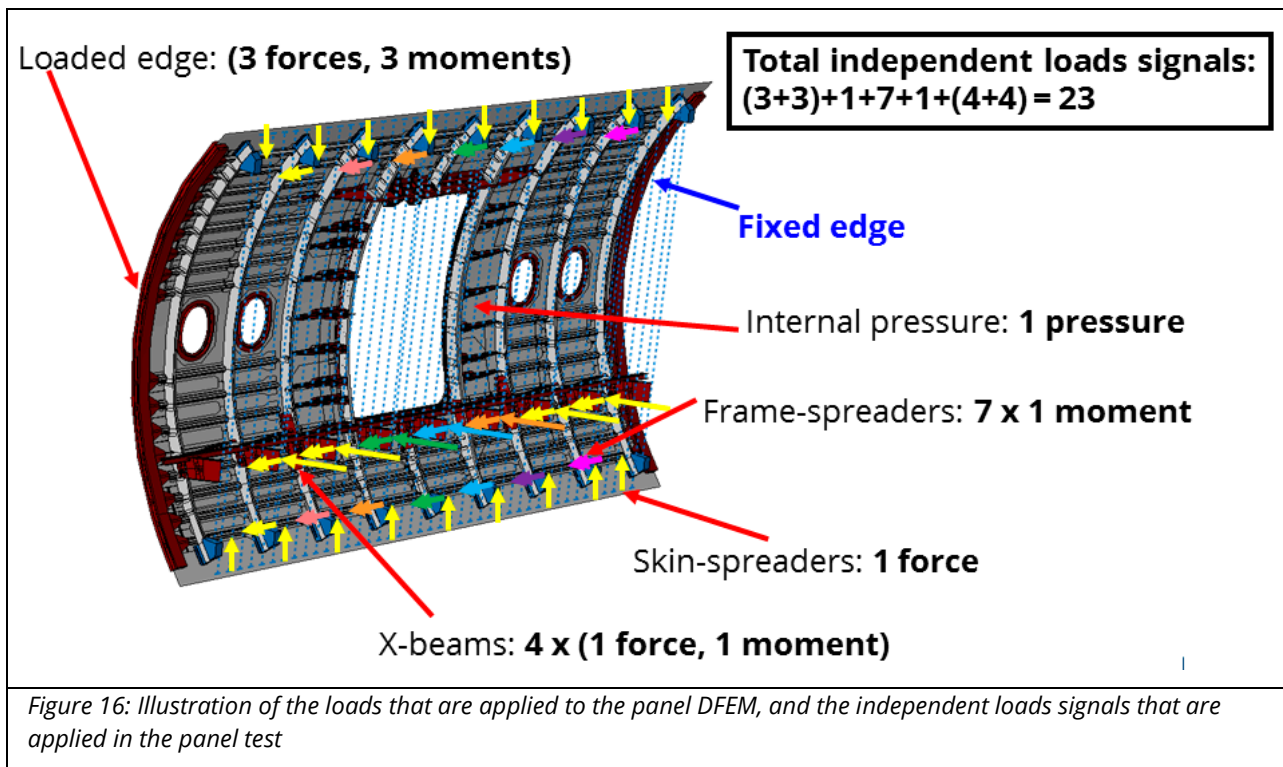
Also the systems from the test rig for the fixation of the panel and the application of the loads (force/moment actuators, internal pressure) are represented in the panel DFEM and accordingly the loads and boundary conditions on the DFEM are prescribed. Most of these systems are simply represented by constraints (suppressed displacements, e.g. the main boundary condition for the panel is the fixation of the right curved edge) and by nodal forces and moments (e.g. for the main bending forces and moments on the left curved edge Figure 14). It should be noted that the large steel structure parts that are mounted on the cross-beams (e.g. see Figure 6) for the force and moment load introductions, are not included in the panel DFEM but simply their resulting force and moment values are prescribed at the cross-beam ends.



Besides the loads that are indicated in Figure 14, some additional loads are also applied to the panel: The so called skin-spreader loads and the internal pressure load. The skin-spreader loads are tension forces between the upper and lower straight skin edges, which compensate for the stiffness of the structure that surrounds the panel in the barrel-test. In total, 42 skin-spreaders are applied, evenly distributed over the length of the straight skin edges (Figure 15). Furthermore, internal pressure is applied to the panel. This is achieved in the test rig by mounting an airtight pressure-box to the panel (Figure 15). This pressure-box is a specific glass-fibre composite component, which is very stiff for pressure loading but very flexible for tension and bending loading. Although the stiffness of this pressure-box is very low compared to the panel, it cannot be neglected and therefore must be included in the virtual test DFEM to account for its effects on the panel responses in the tests.

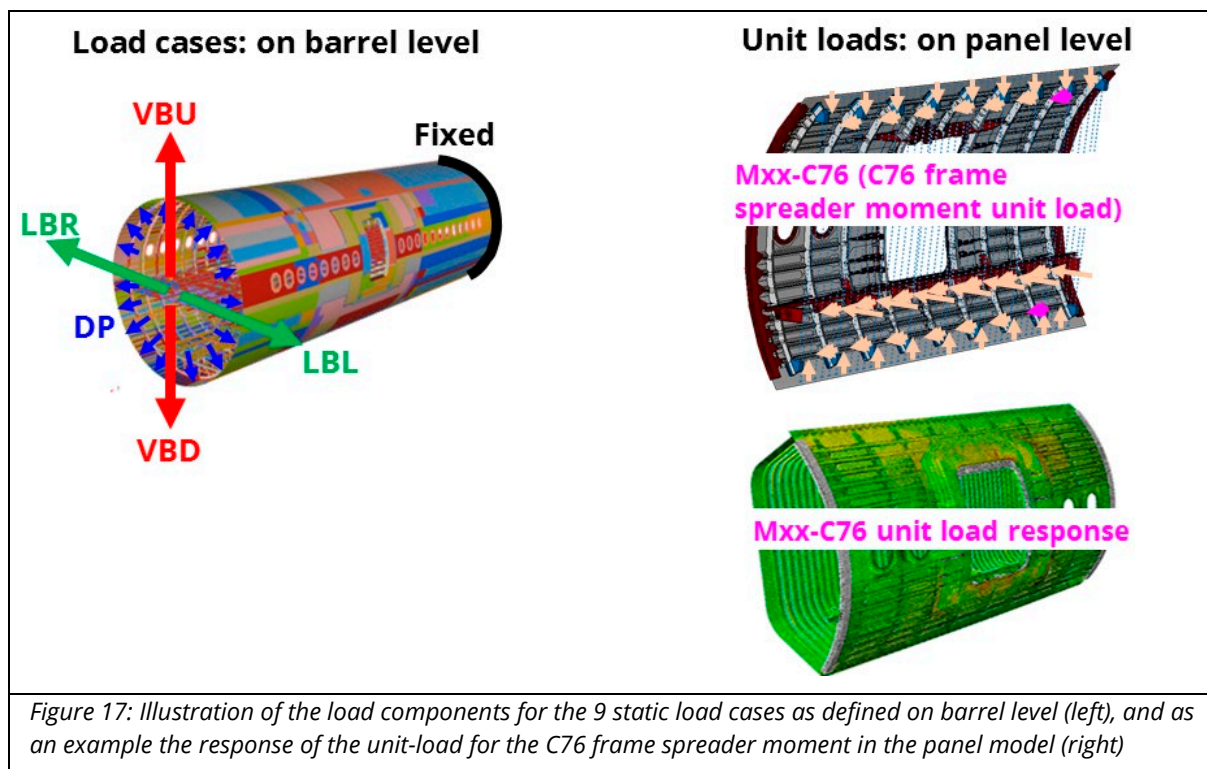


The loads in the panel are applied by the test rig through an extensive set of hydraulic actuators and a pneumatic pressurisation system. These loads shall reproduce, as well as possible, the load distribution from the barrel-level load-cases such as lateral bending, vertical bending and internal pressure. In the test rig, a total of 23 independent load signals are used. Twenty two signals controlling one or several of the hydraulic actuators are used and one signal controlling the pneumatic pressurisation of the panel. The 6 large external hydraulic actuators of the test rig (see Figure 2) deliver the concentrated forces and moments as applied to the panel's loaded edge. I.e. the left curved edge of the panel (see Figure 14) and the right curved edge is fixed. This effectively yields 3 independent forces and 3 independent moments, requiring 6 of the 23 independent load signals. Many other hydraulic actuators, mounted internally in the pressure box, deliver the forces and moments on cross-beams, frame-spreaders and skin-spreaders. In total, 4 independent forces and 4 independent moments are used for the loading of the cross beams, requiring 8 of the 23 independent load signals. Seven independent moment values are used for the loading of the frame spreaders, requiring 7 of the 23 independent load signals. Only 1 independent force value is used for the loading of the skin spreaders, requiring 1 of the 23 independent load signals (Figure 16).



4.5 Load cases and static analyses

The 9 static load cases, which are defined on barrel level, are the combinations of lateral-left and -right and vertical-up and -down bending (LBL, LBR, VBU, VBD) and differential pressure (dP) (Figure 17).



The panel level loads (i.e. the test rig actuator loads) shall be determined for each of these load cases. For this purpose linear static analyses are done of the panel response subject to the unit-loading for each of the 23 independent load signals (Figure 17). These responses are then used in the load identification procedure described below.

4.6 Loads identification

The 23 independent load signals in the test shall be determined such that the deformation of the panel in the test rig is as close as possible to the deformation that would occur in the full-scale barrel test for a given load-case (for example, a vertical bending down (VBD) case). Therefore the barrel DFEM can be used to simulate the deformation that would occur in the full-scale barrel test. From the barrel simulations, large sets of surface strain data (typically including ϵ_{11} , ϵ_{12} , ϵ_{22}) in the panel region of the barrel DFEM can be extracted that are representative for the strains in this region in the full-scale barrel test. Then the 23 independent load signals in the panel DFEM are tuned such that the surface strains in the panel are accurately matched to the strains from the barrel model. A least squares minimisation procedure, minimising the sum of squares of the residuals between the strains in the panel and the barrel is applied to identify the load signals values that best match these strains. For efficiency of the minimisation procedure the superposition principle is applied and therefore the strains coming from linear panel DFEM analyses responses for pre-defined unit-load values for each of the 23 independent load signals are used. Hence linear unit-load analyses are performed for all 23 load signals separately. The resulting (ϵ_{11} , ϵ_{12} , ϵ_{22}) strain responses are collected in all strain locations and are stored in a 23 column-matrix. The least squares procedure determines the linear combination of these columns, i.e. the set of 23 load factors α , that yields the best approximation of the barrel strains, and is expressed in equation 1.

$$\min_{\alpha} \|\epsilon^b - \epsilon^p \alpha\|^2 \rightarrow \alpha = (\epsilon^{pT} \epsilon^p)^{-1} \epsilon^{pT} \epsilon^b \quad (1)$$

Where ϵ^p is the matrix with panel strain values for each of the 23 linear unit-load analyses and ϵ^{pT} is its transpose, ϵ^b is the matrix with the intended barrel strain values, and α is the column with the 23 load factors:

$$\epsilon^p = \begin{bmatrix} \epsilon_{11}^{1,1} & \epsilon_{11}^{1,2} & \dots & \epsilon_{11}^{1,23} \\ \vdots & \vdots & & \vdots \\ \epsilon_{11}^{n,1} & \epsilon_{11}^{n,2} & \dots & \epsilon_{11}^{n,23} \\ \epsilon_{12}^{1,1} & \epsilon_{12}^{1,2} & \dots & \epsilon_{12}^{1,23} \\ \vdots & \vdots & & \vdots \\ \epsilon_{12}^{n,1} & \epsilon_{12}^{n,2} & \dots & \epsilon_{12}^{n,23} \\ \epsilon_{22}^{1,1} & \epsilon_{22}^{1,2} & \dots & \epsilon_{22}^{1,23} \\ \vdots & \vdots & & \vdots \\ \epsilon_{22}^{n,1} & \epsilon_{22}^{n,2} & \dots & \epsilon_{22}^{n,23} \end{bmatrix}; \alpha = \begin{bmatrix} a_1 \\ a_2 \\ \vdots \\ a_{21} \end{bmatrix}; \epsilon^b = \begin{bmatrix} \epsilon_{11}^{1,barrel} \\ \vdots \\ \epsilon_{11}^{n,barrel} \\ \epsilon_{12}^{1,barrel} \\ \vdots \\ \epsilon_{12}^{n,barrel} \\ \epsilon_{22}^{1,barrel} \\ \vdots \\ \epsilon_{22}^{n,barrel} \end{bmatrix} \quad (2)$$

As a validation of the resulting values of these 23 load factors, the strains coming from non-linear analyses of the load-case resulting from the combined 23 load factors for the panel DFEM and the strains coming from non-linear analyses of the barrel DFEM are compared. This procedure can be executed for each of the considered load-cases, including for example vertical and lateral bending and pressurisation. In the present paper we focus on the pressurized vertical bending down (VBDdP) limit-load case, but other load cases (like the un-pressurized lateral and vertical bending up, LBL, VBU) are treated in a similar way.

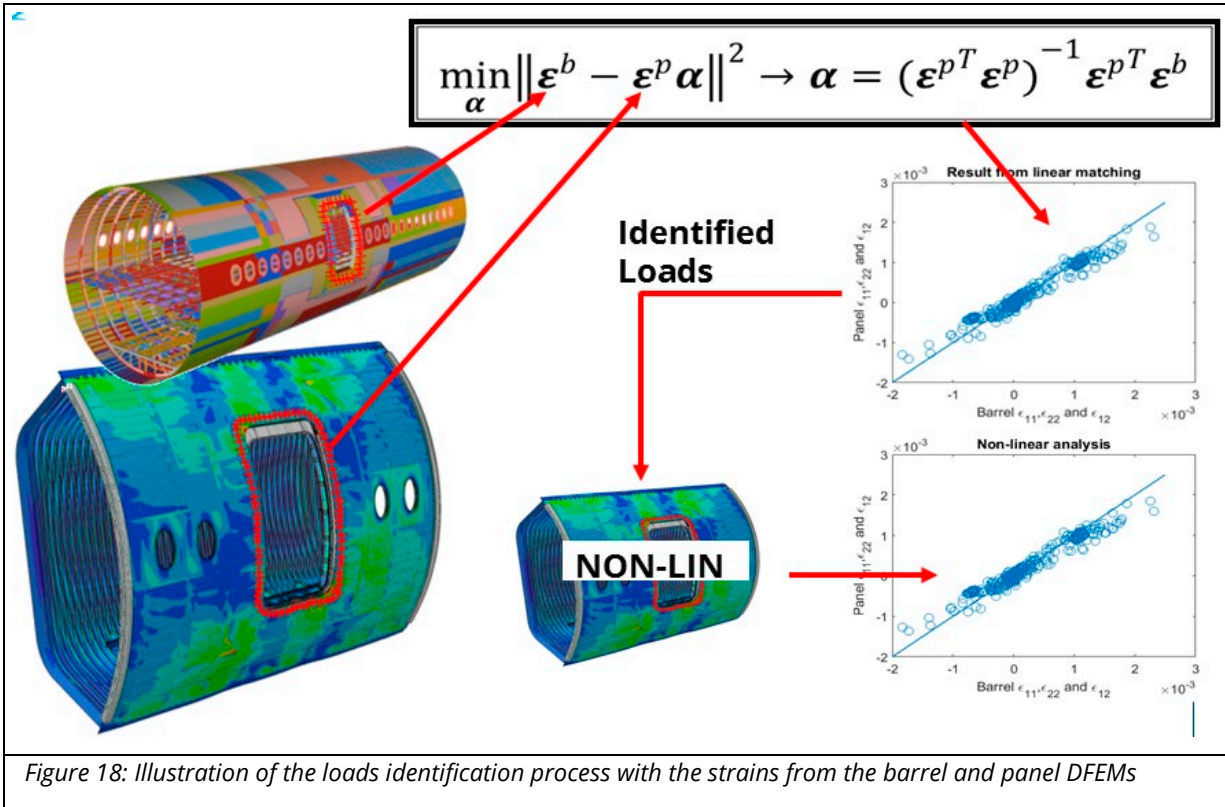


Figure 18: Illustration of the loads identification process with the strains from the barrel and panel DFEMs

The loads identification is based on the matching of strains coming from barrel DFEM and panel DFEM analyses. One sub-set of surface strain locations (at skin surface around the PAX door cut-out) is indicated in the barrel and the panel DFEMs (Figure 18 ; left picture). It should be noted that multiple sets of such strain locations are used in the loads identification procedure. The correlation plots of the

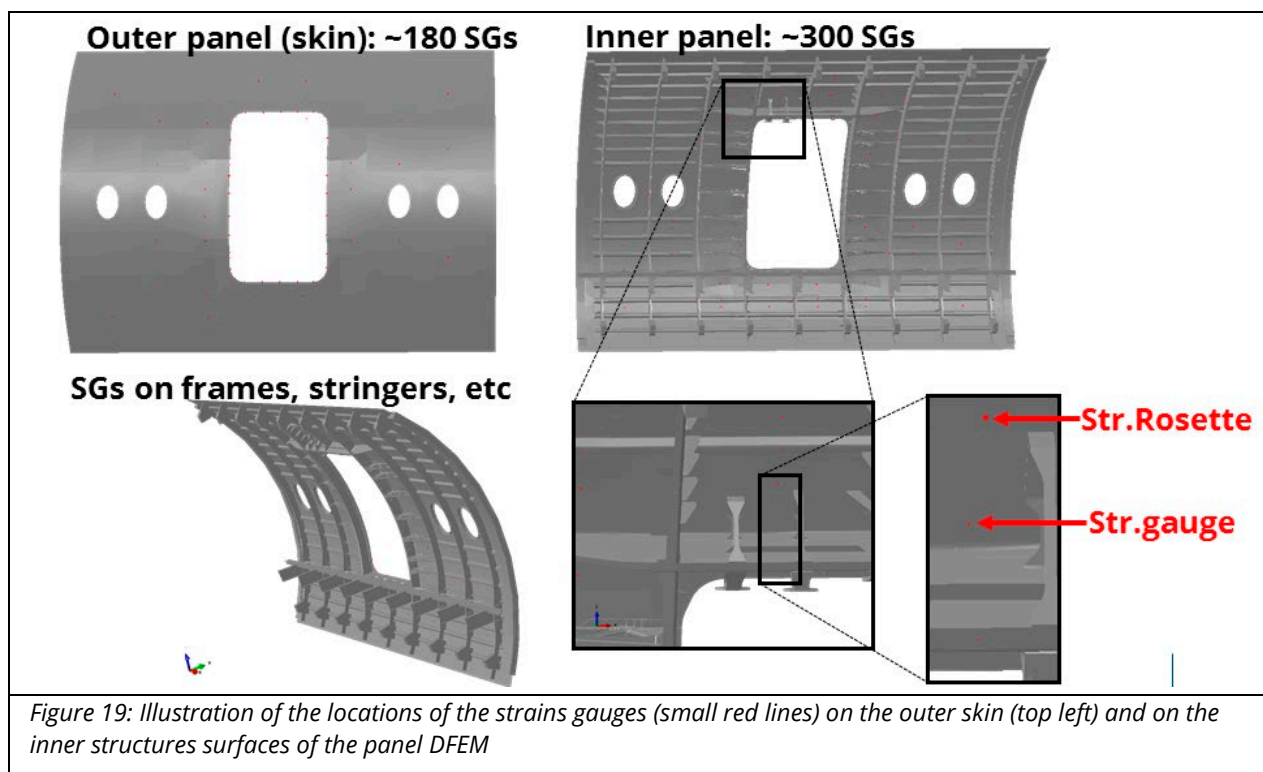
strains from the panel DFEM versus the barrel DFEM, as obtained by least squares minimisation for one of the bending load-cases, are shown in the graphs (horizontal axis: barrel strains; vertical axis: panel strains; upper graph: strains from linear DFEM analyses; lower graph: strains from non-linear DFEM analyses). Apparently the strains from the non-linear DFEM analyses are quite close to the strains from the linear DFEM analyses.

4.7 Strains evaluation

An extensive set of strain gauges is used for the local strain measurements in the test rig. In total about 480 strain gauges are applied. On some of the panel areas of sub-structures that are susceptible to local bending these strain gauges are placed back-to-back and in some areas where strong shear is expected these strain gauges are placed in rosette-formation.

Obviously, with the gauges in rosette-formation it is possible to measure the associated extensional strains in these directions. It must be noted that there is no direct way to measure the shear strain, nor is it possible to directly measure the principal strains since the principal directions are not known. However, these strains can be derived from the rosette strains, using two dimensional strain transformation equations as given in structural mechanics text books (e.g. [7] and [8]).

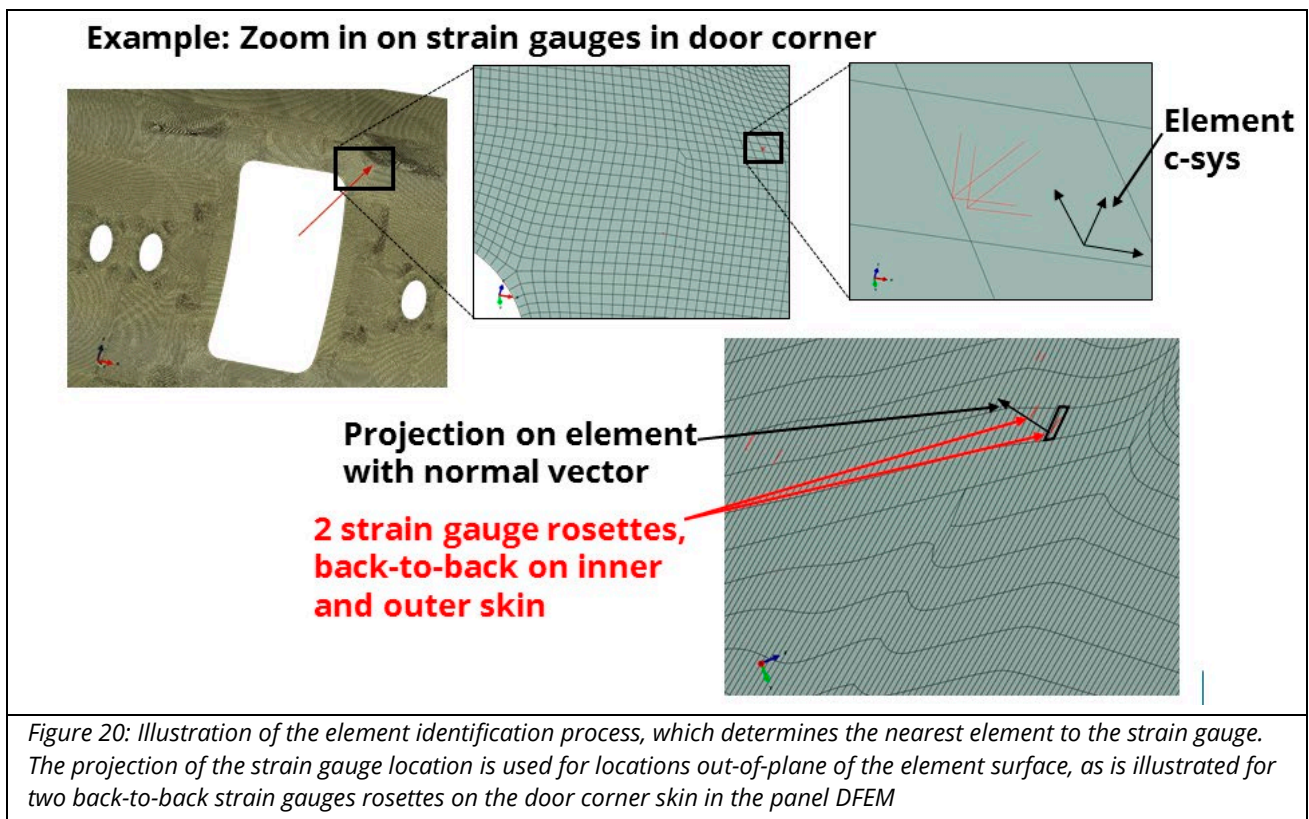
For the correlation of the virtual test analyses results with the responses from the physical tests in the test rig, this complete set of strain gauge responses is also evaluated from the panel DFEM. The incorporation of the strain gauges in the DFEM is illustrated in Figure 19.



The strain gauges response evaluation from the panel DFEM can be achieved in various ways, which will be elaborated a bit in the next section.

4.7.1 Direct strain evaluation

Firstly, the strains can be evaluated from the DFEM analysis result file (ABAQUS .odb file). The first challenge here is to identify for each of the strain gauges exactly the correct element in the panel DFEM. This is not trivial because the strain gauges are located at some (small) distance (up to several millimetres) away from the surfaces of the DFEM part-instances, which is due to small changes in surface definitions from CAD to DFEM and due to simplifications in the DFEM like the mid-surface shell representations of solid CAD parts. Hence the identification of the correct DFEM element to a strain gauge involves the projection of the strain gauge location on the element surface. Moreover, the strain gauges are placed at the upper and/or lower surface of the parts (e.g. the outer and/or the inner surface of the skin), for which the correct corresponding section point in the shell element (e.g. the top or bottom ply in a composite laminate shell element) must be selected. Also, the strain gauges represent the strain in an orientation that is in general not equal to the main axis of the element co-ordinate system so therefore the appropriate strain transformation must be applied to the element strain values. All these aspects are implemented in an automated element search and strain evaluation procedure that is applied to the panel DFEM analysis result file. In this procedure the locations and orientations of the strain gauges are used, which are derived from the strain gauges definitions that are given in the global co-ordinate system of the panel DFEM. Each strain gauge is defined as a line in 3D space by its begin and end co-ordinates, hence the midpoint and the orientation of this line are used as the strain gauge location and orientation, respectively. An example of the element identification process using the projection of the strain gauge locations for two back-to-back strain gauges rosettes on the door corner skin is illustrated in Figure 20. The elements in the DFEM are identified and their strain values evaluated for all the other strain gauges that are located on the skin, frames, stringers, cross-beams and other parts.



4.7.2 Incorporation of strain gauges in DFEM

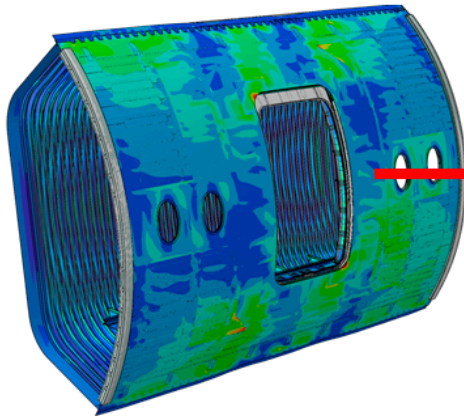
Another approach for strain gauge evaluation requires the incorporation of the strain gauges as structural elements (typically simple linear truss or beam elements with very low stiffness) attached to the structure in the panel DFEM. This approach is commonly used and it yields a proper representation of the strain sensing in the physical test with easy identification and evaluation of the strain gauges responses (i.e. simply by the strain values from the respective set of truss/beam elements). The difficulty with this approach is that the DFEM must be extended with additional part instances (i.e. the strain gauges) that shall be properly attached to the panel structure. This typically can be achieved by tie constraints, but that requires the identification of all the surfaces to which the strain gauges must be tied, which is a tedious and risky operation on the complex panel DFEM. Therefore this approach is not further considered in this study.

4.7.3 Strain gauges as sub-model of the DFEM

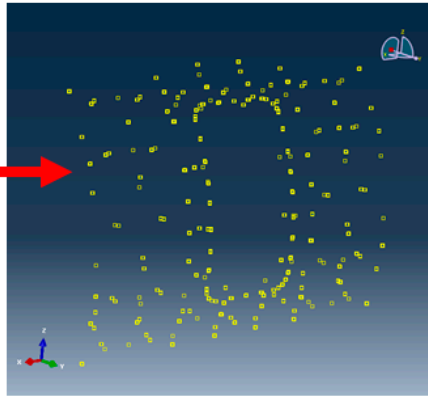
Another approach is to evaluate the strain gauge responses off-line from the panel DFEM analysis. A so-called ABAQUS sub-model is created that contains only the strain gauge elements (e.g. simple linear beam elements with very low stiffness). The boundary conditions (i.e. nodal displacements) for these elements are automatically retrieved from the panel DFEM analysis results (.odb file). ABAQUS provides specific functionality to automatically determine these sub-model displacements from the deformation of the global-model, i.e. the panel DFEM (Figure 21).

Obviously, the strain gauges' strains can be simply extracted from the deformations of the strain gauge elements in the sub-model.

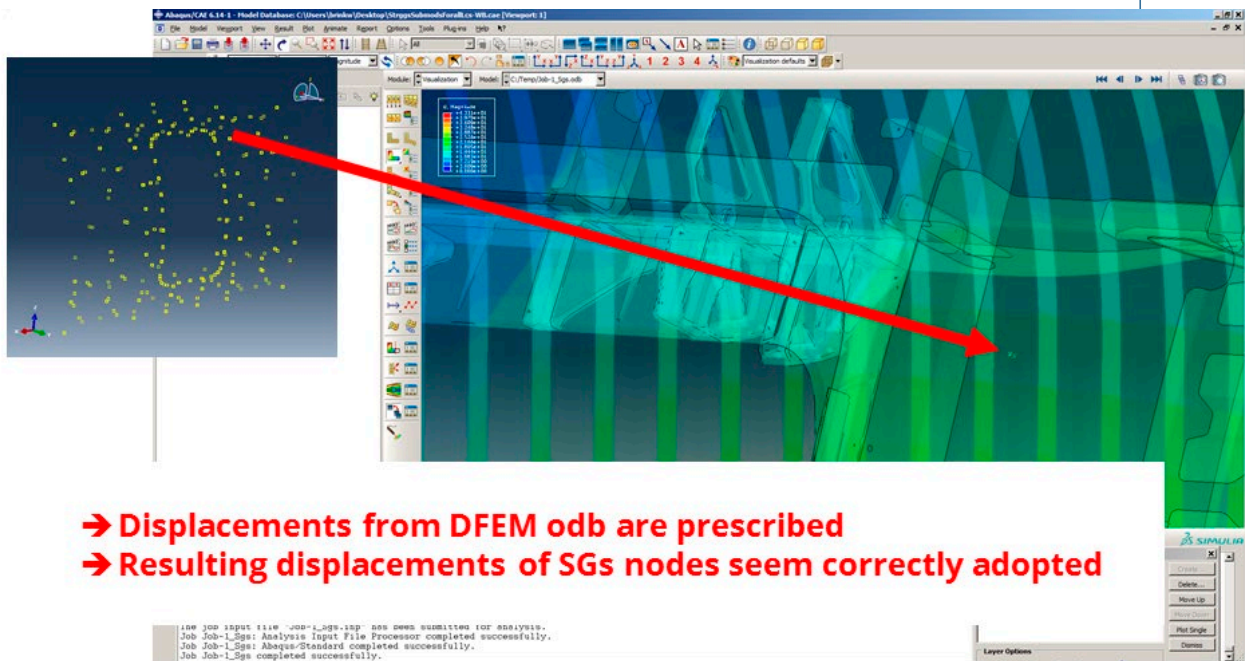
**DFEM analysis result:
Deformation field for certain LC**



**Sub-model with only strain-gauges:
Nodal-displacement BCs for certain LC
derived by Abaqus from DFEM result**



- Only very small/simple model needed
- Just 1 lin. beam el. For each strain gauge
- Element strains directly correspond to test



- Displacements from DFEM odb are prescribed
- Resulting displacements of SGs nodes seem correctly adopted

Figure 21: Illustration of the strain gauges sub-model process: the sub-model (on the right) contains only the strain gauges as linear beam elements. The boundary conditions (i.e. nodal displacements) for these elements are automatically retrieved from the panel DFEM analysis results (on the left) for a certain load case

This approach has been implemented and the strain results are assessed. The correlations between these strains and the strain results from the direct strain evaluation approach are further analysed and compared. These analyses yield to some extent a cross-validation of the strain values from both evaluation methods.

5 Results from strain evaluation study

The correlations between strains in the strain gauges as obtained from the direct strain evaluation and from the sub-model process are further analysed and compared (Figure 23). Note that this concerns only the correlations between the strain gauges predictions as described in section 4.7.1 and in section 4.7.3, and not the strain gauge data from the physical tests because these results are not yet available. Hence the considered correlations are between the strains as derived from the shell elements of the panel DFEM structure (in the direct strain evaluation) and the strains from the strain gauge beam elements (in the sub-model process). The strain correlations are considered for each of the 9 load cases. First, for one load case (VBDdP) only, it is checked if geometrically linear analyses of the DFEM are sufficiently accurate for these strain gauge evaluations. This is done by comparing the strain gauges responses from the linear DFEM analyses with those from the geometrically non-linear DFEM analyses (Figure 22).

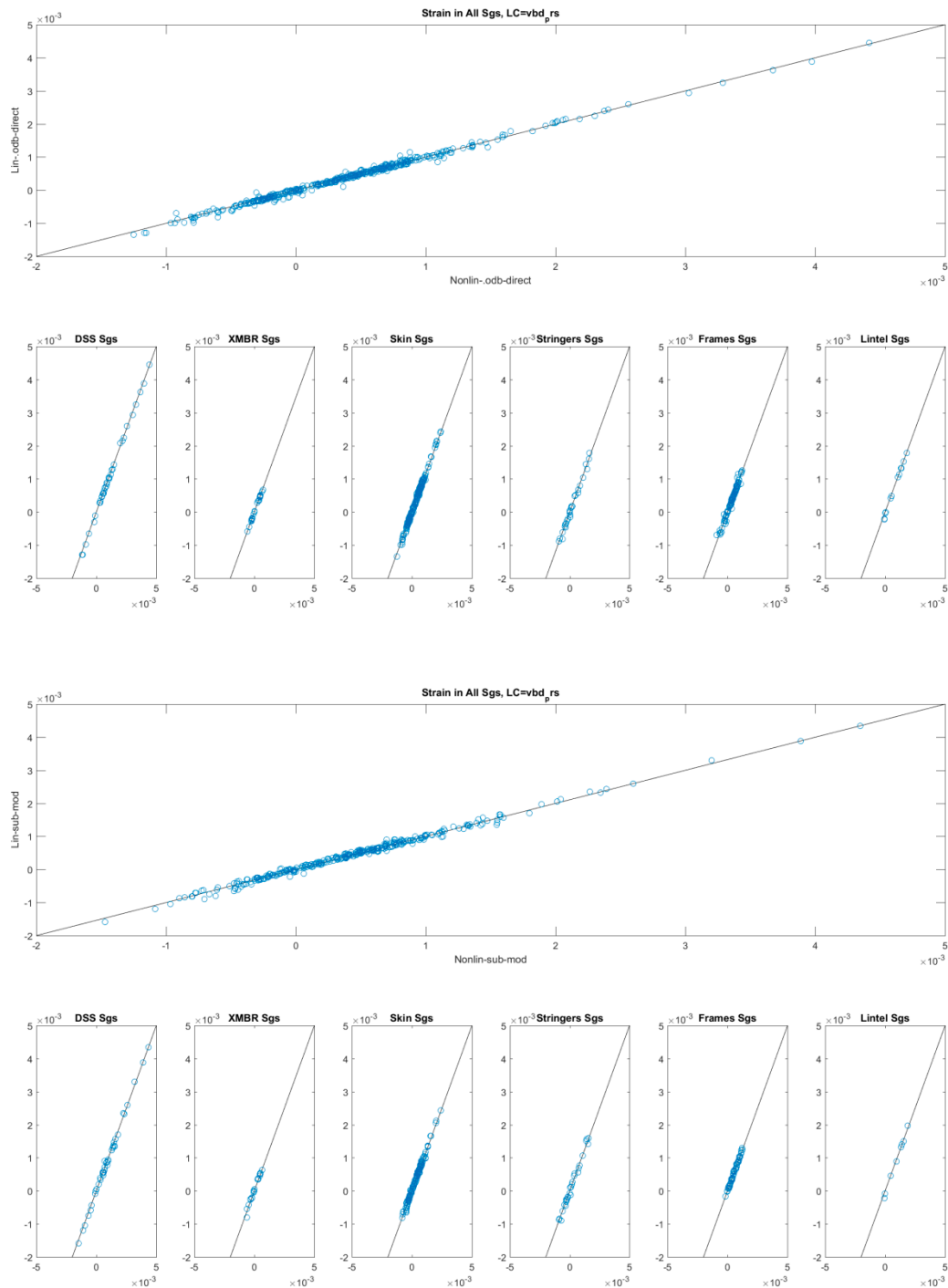
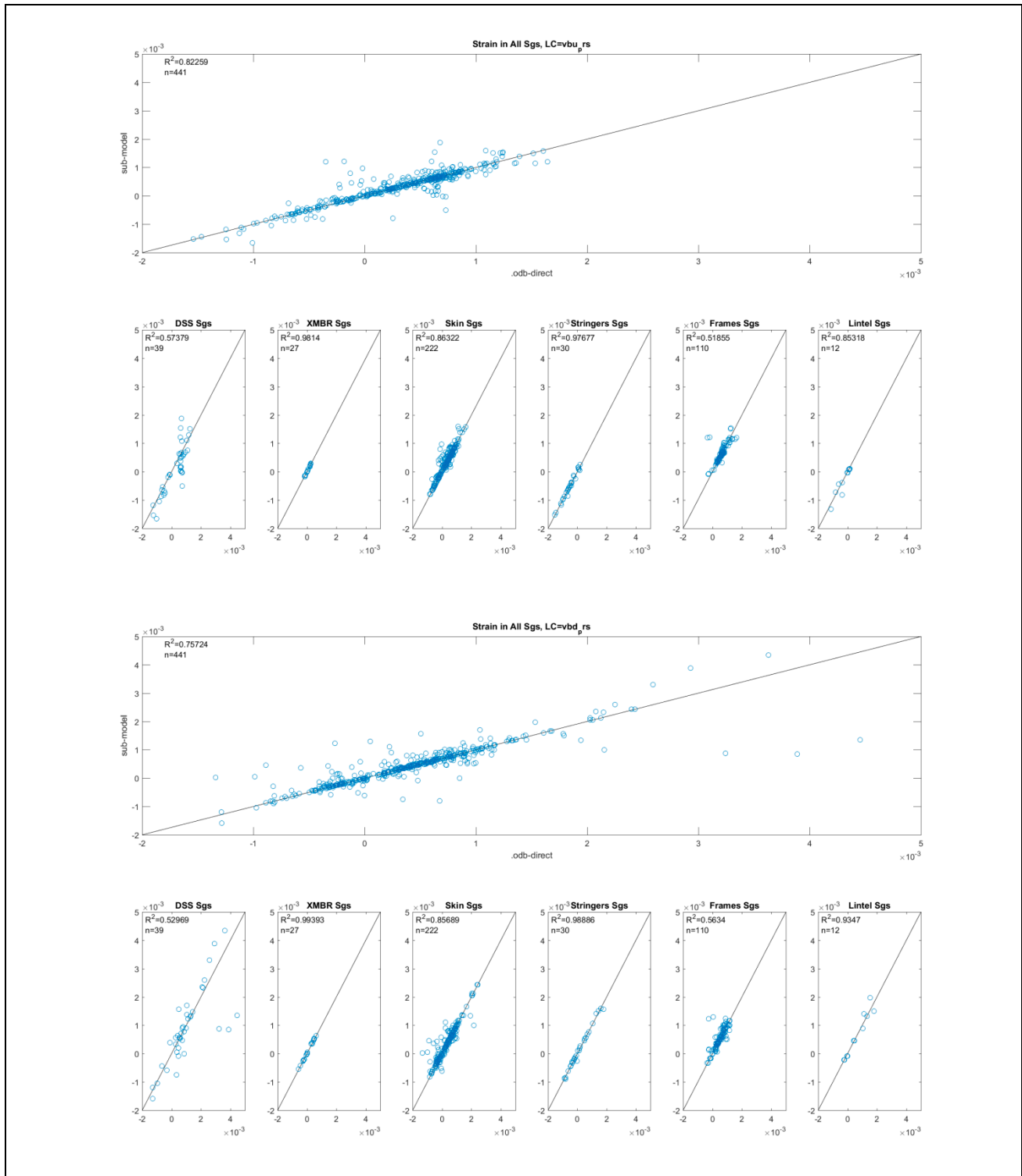
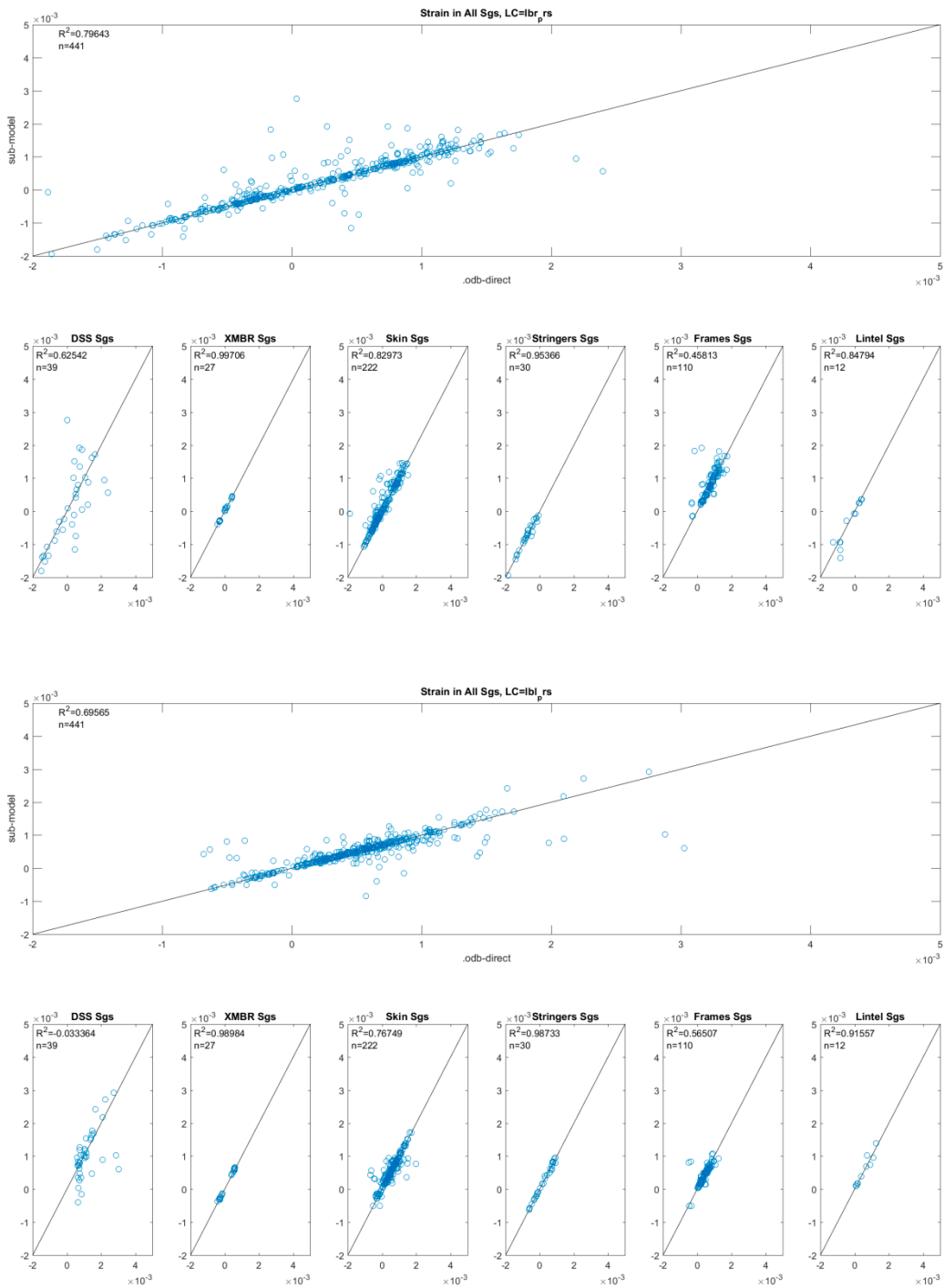


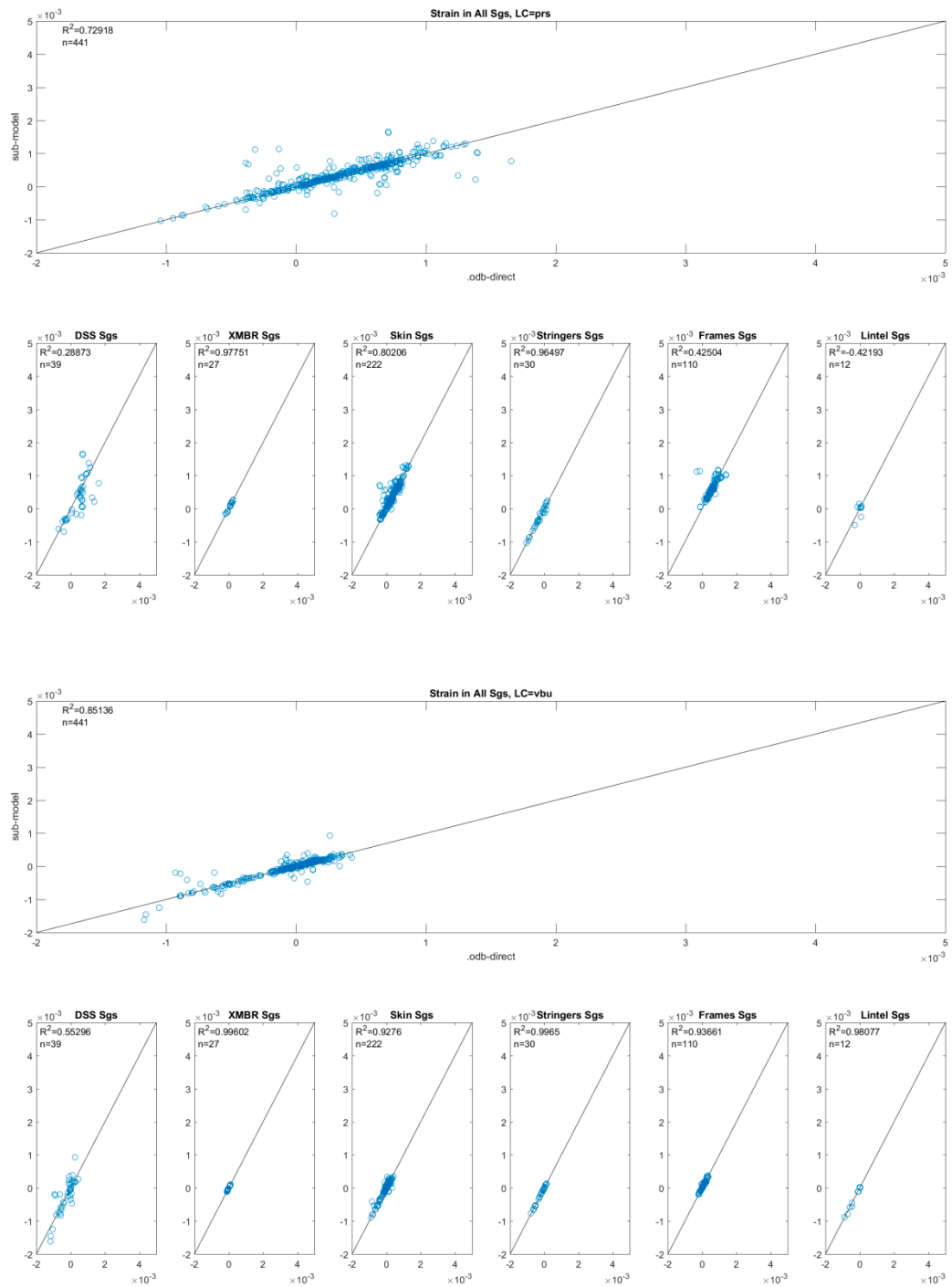
Figure 22: comparison of the strain gauges responses from the linear DFEM analyses with those from the non-linear DFEM analyses. This linear-nonlinear comparison is done for both the methods by which the strain gauge strains were obtained: by the direct .odb evaluation (upper set of plots), and by the sub-model process (lower set of plots)

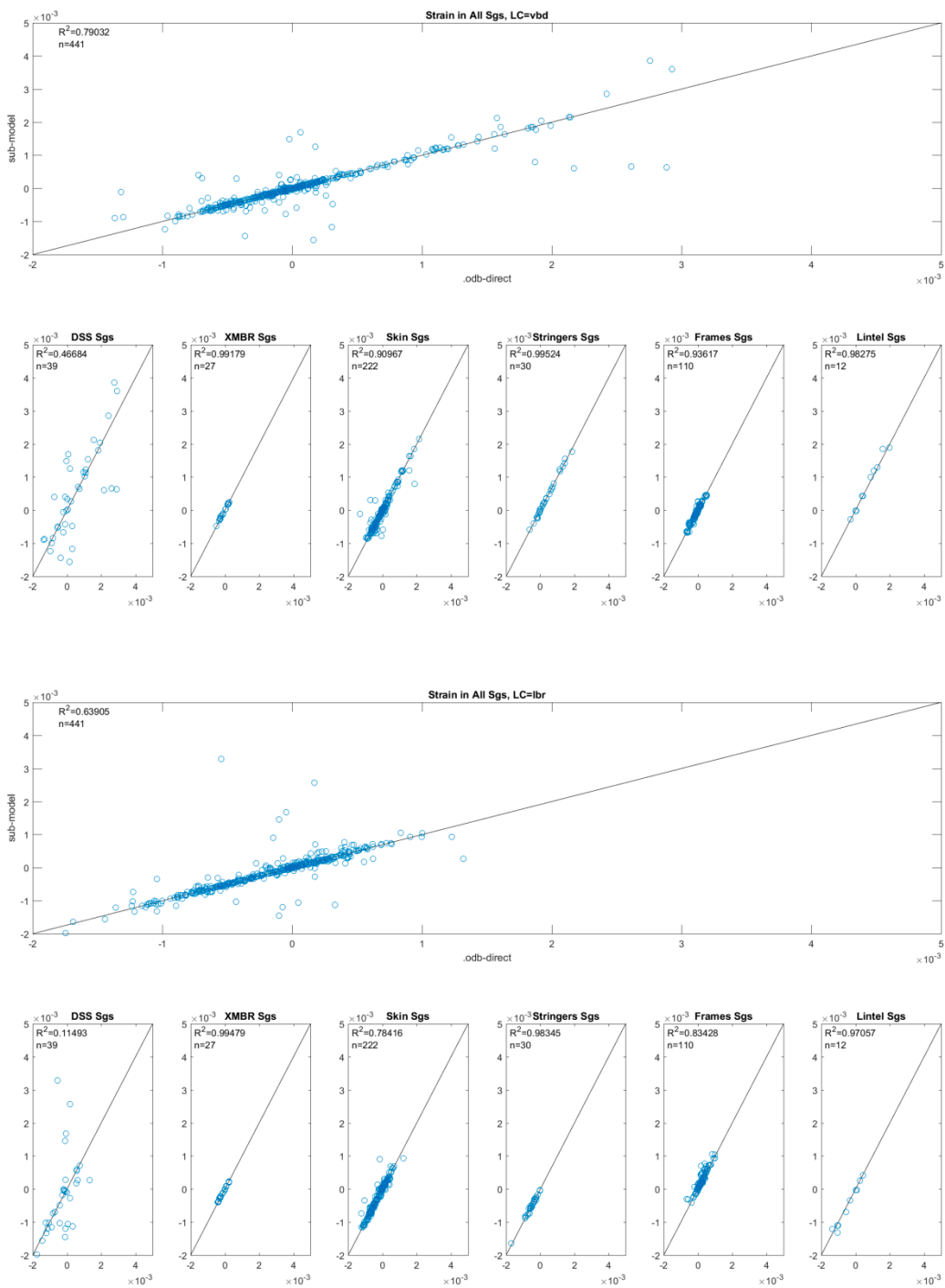
For both sets of strains it is found that the strain values from the linear DFEM analyses are quite similar to the strain values from the non-linear DFEM analyses. Apparently there is only very limited effect on the strains from geometrically non-linear phenomena such as buckling. Therefore it was decided to do only the linear DFEM analyses for the remaining 8 load cases.

The correlations between strains in the strain gauges as obtained from the direct strain evaluation and from the sub-model process for all the 9 load cases are presented below (see Figure 23).









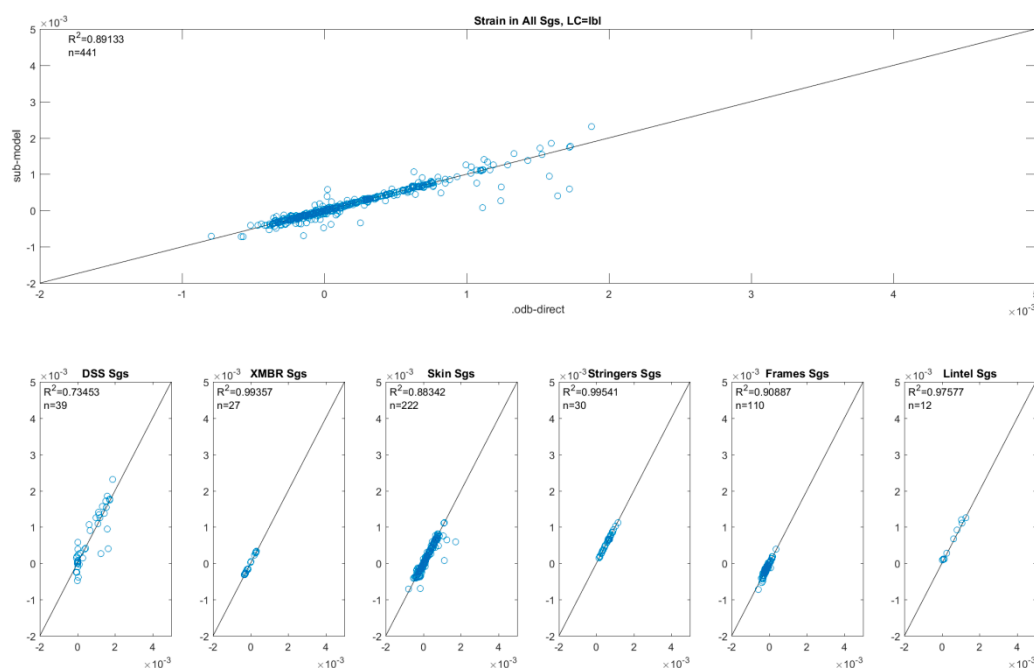


Figure 23: The correlations between strains in the strain gauges as obtained from the direct strain evaluation and from the sub-model process for all the 9 load cases

From these results it is concluded that there is a reasonable correlation between the two methods for the evaluation of the strains in the strain gauges. The statistical quality of the correlation of the strain data sets from all strain gauges as expressed by the coefficient of determination (R^2) varies for the various load cases between 0.64 and 0.89. This gives some indication that for most strain gauges the strains evaluations for both methods are similar and are probably correct. An overview of the R^2 values for each of the load cases is given in the table below.

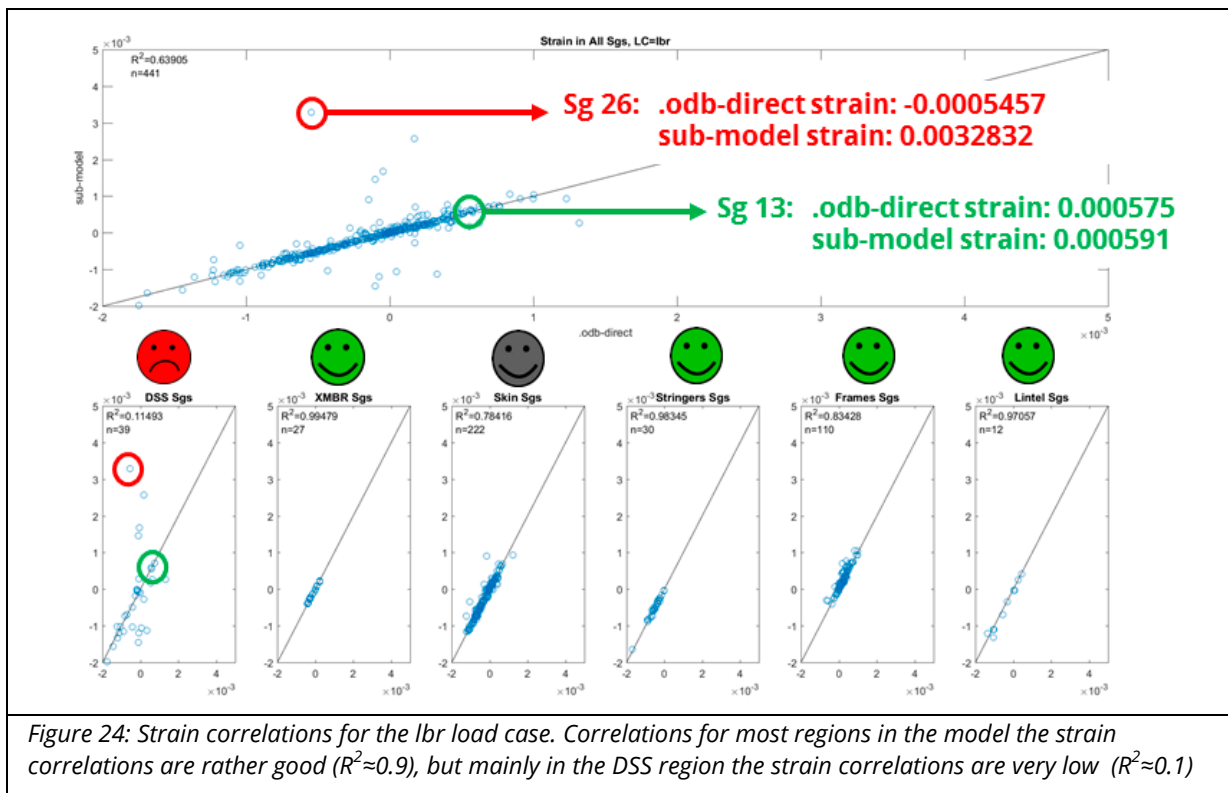
Table 1 Overview of the R^2 values for each of the load cases

LC	R^2
LBL	0.89
LBLdP	0.70
LBR	0.64
LBRdP	0.80
VBD	0.79
VBDdP	0.76
VBUD	0.85
VBUDdP	0.82
dP	0.73

The quality of the correlation depends strongly on where in the model the strains are evaluated:

- for most load cases, the strain correlation is rather good for the strain gauges in the cross members (XMBRS), skin, stringers and lintel;
- in particular the strain gauges in the door surround structure (DSS) have poor correlations, and for some load cases also in the frames. This indicates that there are probably some issues with the strain evaluation in these areas.

If we take a closer look, for example, at the DSS strain correlation for the lbr load case, which has the lowest value for the coefficient of determination ($R^2 = 0.64$), we find that a few specific strain gauges have very low correlations.



For example, for strain gauge nr. 26 (location: $x=8253.785$; $y=2961.28$; $z=24.27$; sub-model-index: 247), the strain values found are very different: .odb-direct strain: -0.0005457 ; sub-model strain: 0.0032832. In comparison, for the DSS strain gauge nr. 13 (location: $x=8256.555$; $y=2520.545$; $z=1897.845$; sub-model-index: 228), the strain values found are much better correlated: .odb-direct strain: 0.000575 ; sub-model strain: 0.000591. These strain gauges are located in different corners of the DSS, see Figure 25.

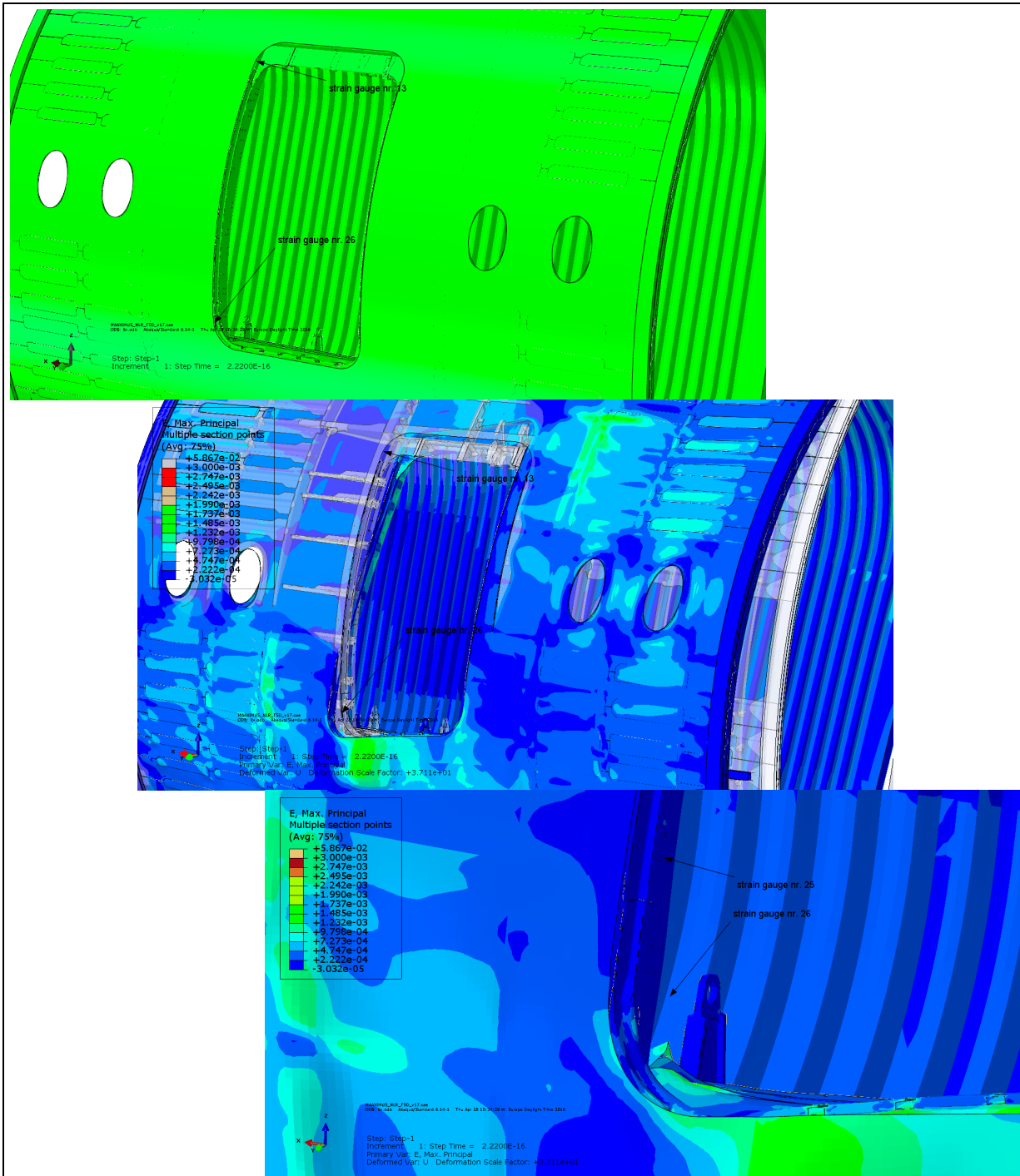


Figure 25: Illustration of the locations of some of the DSS strain gauges: the strain gauges 13 and 26 are located near the inner edge of the door skin and therefore the determination of the correct element strain value is quite error prone

These differences are due to the locations of these strain gauges. In these locations, at the inner edge of the door skin the determination of the correct element strain value is quite error prone. Therefore, these “unreliable” strain gauges have to be identified and carefully checked. The cross-validation procedure with the sub-model strains prediction allows for a relatively easy way to do this identification and checking of strain gauges, and as such this correlation study can help to improve the confidence in the model predictions of the strain gauges strains.

6 Conclusions

This paper presents the development of a detailed finite element model (DFEM) for application in a virtual testing study of a large composite fuselage side panel. Detailed strain data from the DFEM can be used for validation and correlation of the local structural model responses by comparison with the local measurements from the physical tests. The virtual testing modelling methods and evaluation procedures for large sets of strain gauges have been investigated. Several methods for detailed and efficient strain data extraction from large finite element models have been evaluated. The actual comparison of the DFEM strain results with the strain gauge data from the physical test cannot be presented because the test results are not yet available. The focus is therefore on the virtual test analyses.

The results from these different methods for accurate strain data extraction are used for a cross-validation analysis of the strain values from both evaluation methods. It is concluded that there is a reasonable correlation between the two methods (i.e. one by direct strain evaluation and the other from the sub-model process) for the evaluation of the strains in the strain gauges. The strains in some specific parts of the structure, in particular in the DSS, are poorly correlated. This seems to be due to errors in the element selection process in the direct strain evaluation method, but shall be investigated more closely.

Acknowledgement

The research leading to these results has received funding from the European Community's Seventh Framework Programme FP7/2007-2013 under grant agreement n°213371 (MAAXIMUS, www.maaximus.eu).

7 References

- [1] IMA Materialforschung und Anwendungstechnik GmbH, http://www.ima-dresden.de/index.php?ILNK=bauteilpruefung_luftfahrt_flugzeugrumpfschalen&iL=2 (last accessed 20-04-2016).
- [2] Ostergaard, M.G., A.R. Ibbotson, O. Le Roux and A.M. Prior, Virtual testing of aircraft structures, CEAS Aeronaut J, 1:83–103, 2011.
- [3] <http://www.compositesworld.com/articles/thermoplastic-composites-clip-time-labor-on-small-but-crucial-parts> (last accessed 20-04-2016)
- [4] Dassault Systèmes, CATIA product page, <http://www.3ds.com/products-services/catia/> (last accessed 20-04-2016).
- [5] Dassault Systèmes, ABAQUS product page, <http://www.3ds.com/products-services/simulia/products/abaqus/> (last accessed 20-04-2016).
- [6] http://www.hexcel.com/Resources/DataSheets/Prepreg-Data-Sheets/M21_global.pdf (last accessed 20-04-2016)
- [7] Gere, J.M. and S.P. Timoshenko, Mechanics of materials, PWS Pub Co., 1997.
- [8] <http://soliton.ae.gatech.edu/people/jcraig/classes/ae3145/Lab2/strain-gage-rosette-theory.pdf> (last accessed 20-04-2016).
- [9] MAAXIMUS project, www.maaximus.eu (last accessed 20-04-2016).

This page is intentionally left blank.

NLR

Anthony Fokkerweg 2
1059 CM Amsterdam, The Netherlands
p) +31 88 511 3113 f) +31 88 511 3210
e) info@nlr.nl i) www.nlr.nl